AF INSTITUTE OF TECHNOLOGY

EVALUATION OF INTERPOLATIVE MODELING CONCEPTS FOR FATIGUE CRACK GROWTH AT ELEVATED TEMPERATURE

THESIS

Gerald O. Painter, B.M.E.
First Lieutenant, USAF

AFIT/GAE/AA/84D-20

DEPARTMENT OF THE AIR FORCE
AIR UNIVERSITY
AIR FORCE INSTITUTE OF TECHNOLOGY

Wright-Patterson Air Force Base, Ohio

AFIT/GAE/AA/84D-20

EVALUATION OF INTERPOLATIVE MODELING CONCEPTS

FOR FATIGUE CRACK GROWTH AT ELEVATED TEMPERATURE

THESIS

Gerald O. Painter, B.M.E.
First Lieutenant, USAF

AFIT/GAE/AA/84D-20

Approved for public release; distribution unlimited

AFIT/GAE/AA/84D-20

EVALUATION OF INTERPOLATIVE MODELING CONCEPTS FOR FATIGUE CRACK GROWTH AT ELEVATED TEMPERATURE

THESIS

Presented to the Faculty of the School of Engineering

of the Air Force Institute of Technology

Air University

In Partial Fulfillment of the

Requirements for the Degree of

Master of Science in Aeronautical Engineering

Gerald O. Painter, B.M.E.

First Lieutenant, USAF

December 1984

A-1

Approved for public release; distribution unlimited

Acknowledgements

I am deeply grateful to my thesis advisor, Major George Haritos for his advice during my thesis effort and his patience in proof reading my work. His suggestions have made my work more complete, and I know more readable.

I would also like to thank several members of the Air Force Materials Laboratory and the team from the University of Dayton Research Institute, who work there. My most sincere gratitude, I give to Dr. Theodore Nicholas, who always had the time to sit and advise me. He was always polite and gracious, even when he was pressed with other business. I wish to thank Dave Maxwell for doing such a fine job with the experimental program, and for answering my questions about it. I would like to thank Jim Larsen for his help with the SINH model. Each person I delt with at the Materials Lab helped me whenever I needed it, and they did it cheerfully.

Finally, I would like to thank my wife, Florinda, for understanding why I neglected her during this phase of my life, and my children for understanding why I couldn't always play with them.

Table of Contents

List of Figures

Figure		Page

Abstract

This work presents an examination of interpolative schemes for fatigue crack growth at elevated temperature (1200 F). An interpolative scheme involving the linear superposition of effects due to stress ratio, loading frequency, and peak load dwell or hold time, is applied to two state-of-the-art crack growth rate prediction models. These models are the SINH model, developed by Pratt and Whitney Aircraft, and the MSE model, developed by General Electric. SINH is based on the hyperbolic sine function, and MSE is based on a sigmoidal equation.

The results of an experimental program are presented. Fatigue crack growth rate tests are performed on compact tension specimens according to ASTM standards. Two interpolative models are developed from the resulting data base. Additional tests are performed and the model predictions are compared to these additional tests.

It is found that linear (on log-log scale) functional forms can be assumed to relate model constants to the test parameters (load ratio, frequency, and hold time). Also, it is found that these functional forms can be applied to both models. More work is needed to determine whether the effects of variations in each of the test parameters on crack growth rate are independent of each other and can be linearly superimposed.

When the same functional forms are applied to the SINH and the MSE models, they behave much alike.

EVALUATION OF INTERPOLATIVE MODELING CONCEPTS FOR FATIGUE CRACK GROWTH AT ELEVATED TEMPERATURE

I. Introduction

Background

Changes have been recently made in the United States Air Force design and maintenance philosophies. These new philosophies have created a requirement for more accurate fatigue-crack-growth-rate prediction models for structural alloys used in modern gas-turbine engines. The Engine Structural Integrity Program (ENSIP), and the Retirement For Cause (RFC) Program are two Air Force Programs which embody these new philosophies (1).

ENSIP specifies how future jet engines will be designed. The ENSIP design philosophy is based on the assumption that fatigue cracks exist in new engine components at the time of production. It then becomes part of the design process to demonstrate that these cracks will not grow to catastrophic size during the design life of the engine. During the 1960's, critical engine components were limited by creep and stress rupture phenomena. However, the lives of today's critical engine components are primarily limited by low-cycle-fatigue damage. With this new emphasis on fatigue phenomena, crack growth prediction has become an integral part of the engine design process.

RFC is a component-life management philosophy which seeks to safely utilize a greater portion of the lives of rotating engine parts, and thereby realize considerable economic savings. Consider a typical turbine engine disk. The previous approach had been to use a lower bound on the Low-Cycle-Fatigue (LCF) life which was so conservative that it resulted in 999 out of 1000 disks being retired while still structurally sound. Under the current RFC approach, disks are removed for periodic inspection and returned to service if no cracks larger than a specified detectable size are found. Here is where an accurate crack-growth-rate prediction capability is indispensable. An analysis must be able to demonstrate that cracks of the detectable size and smaller will not grow to catastrophic size during the next inspection interval.

Scope

Most current fatigue crack growth models are of the form

$$da/dN = f(\Delta K) \tag{1}$$

where da/dN is the crack growth rate and ΔK is the stress intensity factor range. If ΔK is to be a valid modeling parameter, Linear Elastic Fracture Mechanics (LEFM) must hold (2). This means that the plastic zone surrounding the crack tip must be small when compared to the crack length. At elevated temperatures one would expect time-dependent material behavior resulting in large scale plasticity and creep damage. However, several investigators (see e.g. Larsen (1,3)) have shown that the ΔK-analysis is valid for nickel-base superalloys for temperatures up to 1350 F.

The goal of this thesis is to determine the effectiveness of state-of-the-art models in predicting crack growth rates for high temperature applications. An examination of two representative examples of current crack-growth-rate predictive models which use ΔK as a correlating parameter is presented. Both of the models are empirical in nature since accuracy requirements for design exceed the predictive capability of any existing analytic description. The two models examined were developed by aircraft engine designers Pratt and Whitney (PW) and General Electric (GE).

PW's model (SINH) uses the hyperbolic sine function to fit the basic sigmoidal shape exhibited by da/dN versus ΔK data, while GE's uses a modified sigmoidal equation (MSE). Both models are discussed in detail in Section III.

This thesis seeks to investigate how well crack growth rate models perform when they have been developed from a minimal data set. The approach taken in this thesis was to collect a minimal set of data at high temperature (1200°F), varying three test parameters: stress ratio, frequency, and hold time. These data were used to formulate predictive models for both the SINH and the MSE equations. Finally, additional data were collected and compared with the SINH and MSE predictions to assess the interpolative capabilities of the models.

It has been demonstrated that both the SINH and the MSE equations do a reasonable job of fitting da/dN versus ΔK data (4). This thesis differs from previous work in that it attempts to test the validity of models in which more than one of the test parameters are allowed to vary at any one time. In their current states of development, both the SINH and the MSE models cannot treat these combined effects in a systematic manner suitable for application to a variety of materials. The version of PW's SINH program described in (5) can only be used to develop interpolative models in which only one test parameter is varied at a time. GE's MSE model as implemented in (6) is not a general purpose model. While it allows more than one test parameter to change at a time, it uses ad hoc functional relationships based on a large data set for one specific material. Therefore, it does not attempt to produce general functional relationships which are valid for a range of materials, as SINH does.

In this thesis, two models are developed for IN718. The experimental program used in the development of these two models is described in Section II. One of the models uses the SINH equation, and the other uses the MSE equation. Both models function similarly. Given a set of test parameters (load ratio, R, frequency, ν, and peak-load hold time, t_H), the models predict da/dN versus ΔK curves.

Data collection for fatigue crack growth modeling is expensive and can take several days to perform. Therefore, in order to reduce the size of the test matrix and the overall complexity of the modeling task, the temperature was held constant. All data were collected at 1200°F. Thus temperature was eliminated as an independent variable, reducing not only the total number of test runs required, but also the number of computer runs necessary to reduce the data and formulate a model.

Fundamental Assumptions

In both the SINH and the MSE models, da/dN is related to ΔK through a set of constants; SINH uses four constants while MSE uses six. When these models were developed, there were several assumptions made concerning the experimental parameters and associated constants. These assumptions are suggested in the SINH documentation (3), but are not fully implemented in the SINH computer program. They have never been applied to the MSE equation prior to this work. The following assumptions are made in this thesis, and they apply to both the SINH and the MSE models for IN718 developed:

1. Constants are related to the test parameters through relationships which are linear when plotted on log-log graph paper.

2. Constants are functions of ν, t_H, R, and T, where ν is loading frequency, t_H is load-dwell time, R is the ratio of minimum to maximum load, and T is temperature.

3. First order dependencies were assumed, i.e., it is assumed that linear superposition holds, and that there are no second order and higher effects.

The purpose of this thesis is not to attempt to justify these assumptions, but rather to examine their validity, and to suggest possible improvements.

II. Experimental Program

Computer-controlled constant-load-amplitude, fatigue crack-growth-rate tests were performed according to ASTM Standard E 647-81. The experimental program was performed at the Air Force Materials Laboratory. This section describes the experimental apparatus, identifies the test matrix and procedures, and outlines the data-reduction techniques employed.

Experimental Apparatus

A closed loop computer-controlled test system was used to collect da/dN versus ΔK data. A block diagram of the test setup is shown in Figure 1. The primary components of the system are an IBM PC microcomputer, an MTS Material Test Frame, a Wavetek Function Generator, and various Analog to Digital (A/D) converters and signal smoothers. Data are taken automatically and minimal human intervention is required.

Figure 2 shows the two raw data items that were actually measured by the test set-up. Crack Opening Displacement's (COD) are measured using an MTS electro-mechanical extensometer with quartz rods for specimen contact, while the loads are provided by an MTS servo-hydraulic load frame, as controlled by the computer. The specimens are enclosed in an electrical resistance furnace to achieve the required elevated temperature.

Test Matrix

A three-dimensional representation of the test matrix is shown in Figure 3. Each of the test variables is plotted on a separate axis.

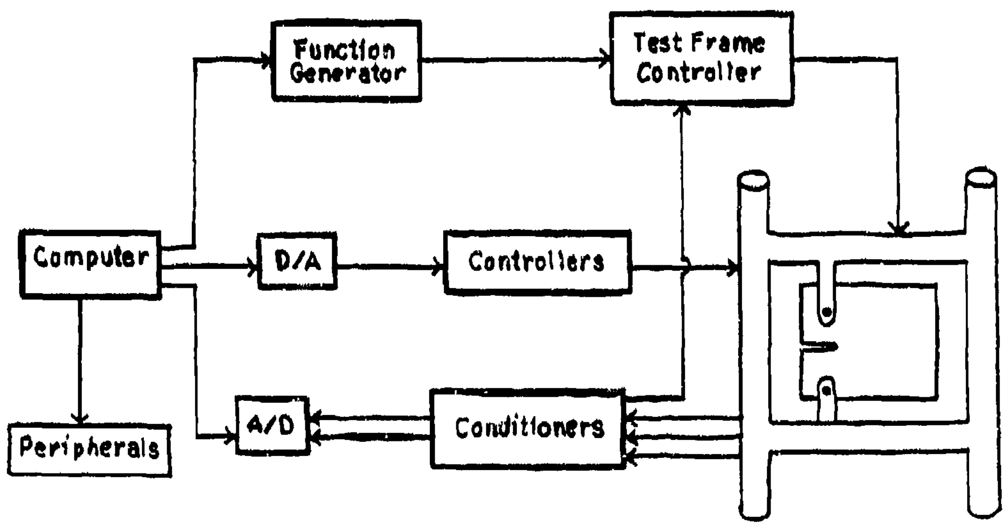

Figure 1. Block Diagram of Test Setup

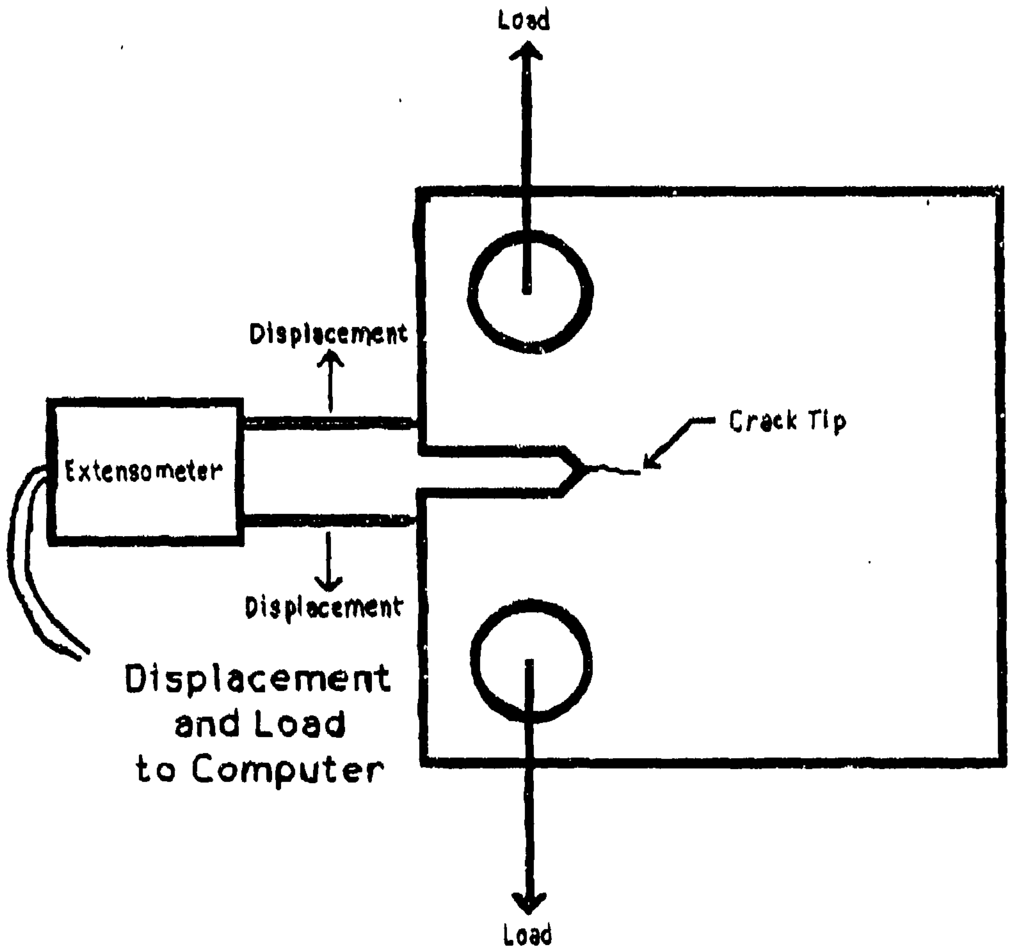

Figure 2. Data Acquisition Process

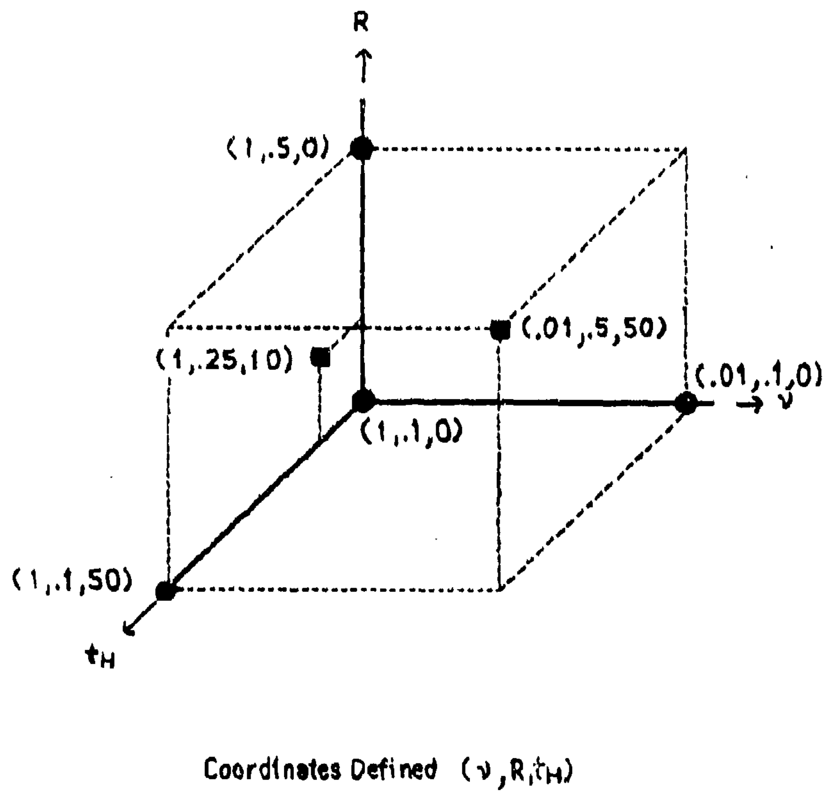

Figure 3. Graphic Representation of Test Matrix

The four points plotted as solid circles represent the four tests used in formulating the predictive models. The coordinates of each point are the values of the test parameters for that particular test. The two points plotted as squares represent the two proof tests which were performed to evaluate the predictive capability of the models. The point at the origin of the coordinate axes represents the baseline test. Moving from the baseline outward along any axis, changes only the value of the variable represented by that axis. Thus, the three points lying on the axes away from the origin represent tests in which only one test parameter is changed from the baseline value. All six tests were performed at a temperature of 1200 degrees Fahrenheit.

Specimen Description

Specimens used for this experimental program were machined from plates of INCONEL 718. IN718 is a nickel-base super alloy with a high fracture toughness, and is commonly used in the fabrication of jet engine hot-section parts. IN718 was chosen as the specimen material because of its utility to the Air Force, and because the MSE model had previously been applied only to AF115. By using a material other than AF115, it could be determined if the functional relationships implicit in the MSE model could be applied to other materials. The specimen geometry is in accordance with ASTM Standard E 647-81 (7), and is shown in Figure 4. The notch which is used to start the crack was cut using Electrical-Discharge Machining (EDM).

Procedure

The specimens were pre-cracked in accordance with ASTM Standard E 399 (8) until a measurable crack extension was observed, with

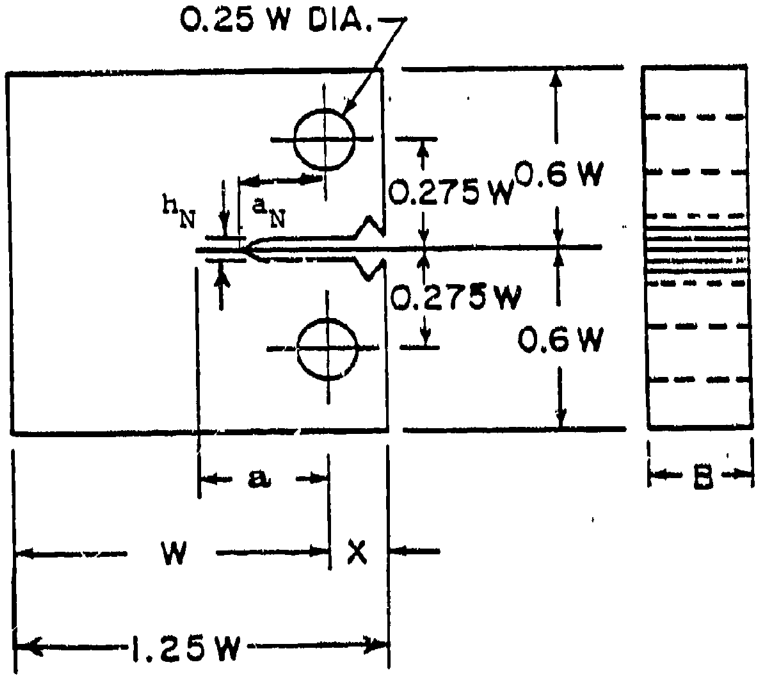

Figure 4. Compact Tension (CT) Specimen Geometry

the final pre-cracking K_{max} being smaller than the starting K_{max}. As suggested in ASTM E 647-81, K_{max} was not changed by more than 20% in any one increment so as to establish a steady-state crack growth rate before taking a measurement. Data were taken automatically with the equipment described. Crack length was derived from compliance using a relationship obtained from a polynomial fit to a series of numerical finite element solutions. By performing a series of finite element calculations for the compact tension (CT) specimen at different crack lengths, a relationship between crack length and compliance can be obtained. This is the method currently in use at the Air Force Materials Laboratory. For a discussion of the error inherent in this procedure see (9). This crack length expression as given in (9) is:

$$\bar{a} = 1.0010 - 4.6695U^{-1} + 18.46U^{-2} - 236.82U^{-3} + 1214.9U^{-4} - 2143.6U^{-5} \quad (2)$$

where $U = (EBV/P)^{1/2} + 1 = (EBC)^{1/2} + 1$

and

a = average crack length (inches)

W = specimen width (inches)

B = specimen thickness (inches)

E = Young's Modulus (psi)

V = crack opening displacement (inches)

P = load (inches/pounds)

C = V/P = compliance (pounds).

The crack length-compliance relationship was calibrated at the beginning of each test by taking a few visual crack-length measurements, and then adjusting Young's modulus, E, in Equation 2.

The stress intensity range ΔK was determined from the ASTM expression as follows (7):

$$\Delta K = \frac{\Delta P}{B(W)^{1/2}} \frac{2 + a/W}{(1-a/W)^{3/2}} [0.866 + 4.64(a/W) - 13.32(a/W)^2 - 5.62(a/W)^3] \qquad (3)$$

where

ΔP = load range, $(P_{max} - P_{min})$

Note that the above expression assumes a linear-elastic, homogeneous test material.

Data Reduction

ASTM Standard E 647-81 suggests two methods for computing crack-growth rates: the Secant method and the Incremental Polynomial Method. The Incremental Polynomial method was used in this experimental program, because it offers some smoothing of the data. In this method, crack-growth rates are computed from crack length versus number of cycles (a versus N) data using a seven-point sliding polynomial curve fitting technique. This technique gives $\hat{a}_i$ and $(da/dN)_{\hat{a}_i}$ by the following expressions:

$$\hat{a}_i = b_0 + b_1[(N_i - C_1)/C_2] + b_2[(N_i - C_1)/C_2]^2 \qquad (4a)$$

$$(da/dN)_{\hat{a}_i} = b_1/C_2 + 2b_2(N_i - C_1)/C_2^2 \qquad (4b)$$

where

$$-1 \le [(N_i - C_1)/C_2] \le +1$$

and

b_0, b_1, and b_2 = constants determined by least squares regression

$C_1 = (N_{i-3} + N_{i+3})/2$

$C_2 = (N_{i+3} - N_{i-3})/2$

$\hat{a}_i$ = fitted crack length

$(da/dN)_{\hat{a}_i}$ = the crack growth rate associated with $\hat{a}_i$ and N_i.

III. Crack Growth Interpolative Modeling

Typical da/dN versus ΔK data plotted on log-log graph paper has a sigmoidal shape as can be seen in Figure 5. The curve is characterized by a slow crack-growth region (I), called the threshold region, a linear region (II), and a rapid growth region (III). Data do not usually extend into region III because test specimens tend to break soon after having entered this region.

If all of the test parameters were held constant with the exception of one, say R, variation of this parameter would generally result in a shifted da/dN versus ΔK curve. The general trends for these curve shifts, for a material with high fracture toughness, such as IN718, can be seen in Figure 6 (3,10). Figure 6a shows that increasing ν will result in a decrease in da/dN for a fixed value of ΔK. Figure 6b shows that increasing R will result in an increase in da/dN for a fixed value of ΔK. It is the goal of crack-growth interpolative models to be able to predict these curve shifts with reasonable accuracy, from a relatively small experimental data base. What follows is a description of the two interpolative models examined in this work, and how they were applied.

SINH Model

Pratt and Whitney's SINH crack growth rate interpolative model is based on the hyperbolic sine function (3,5), as plotted in Figure 7. Its shape closely approximates the sigmoidal shape of da/dN versus ΔK data shown in Figure 5. With the addition of some controlling constants one can force the hyperbolic sine function to fit may possible

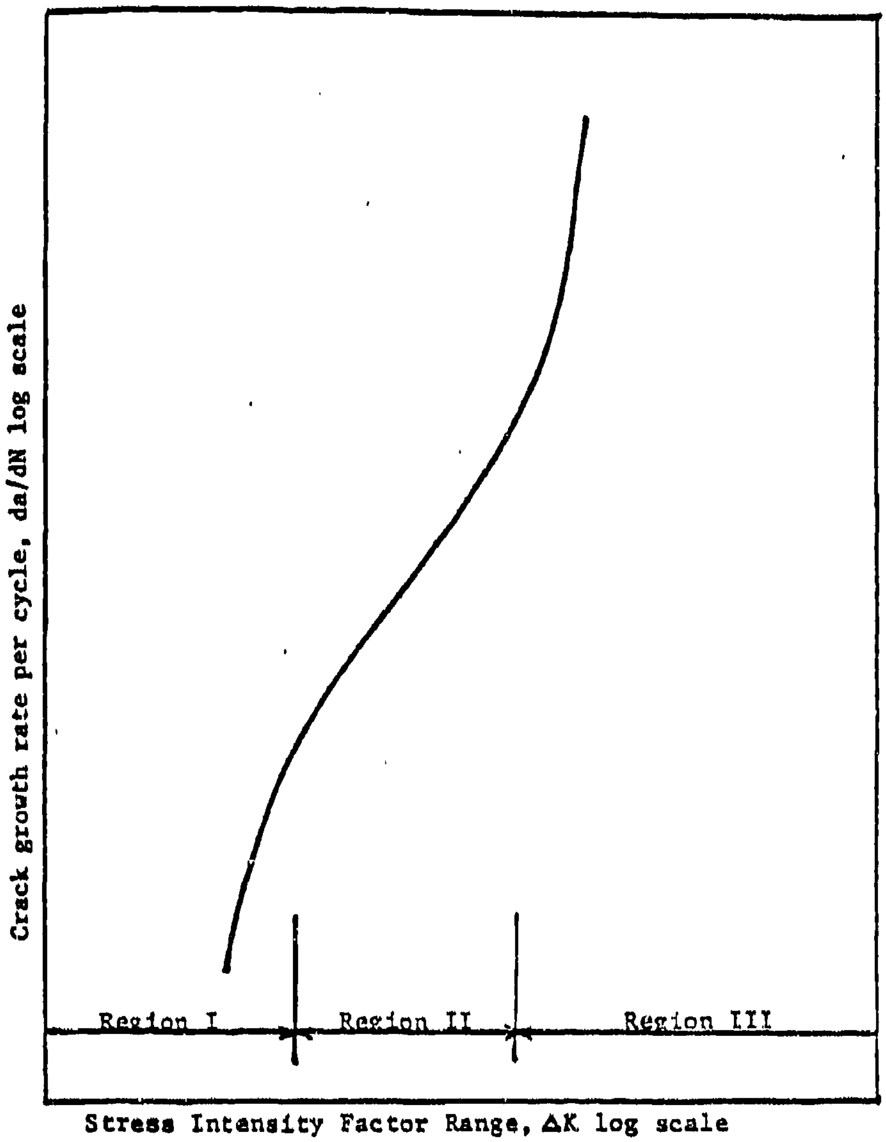

Figure 5. Form of da/dN Versus ΔK Data

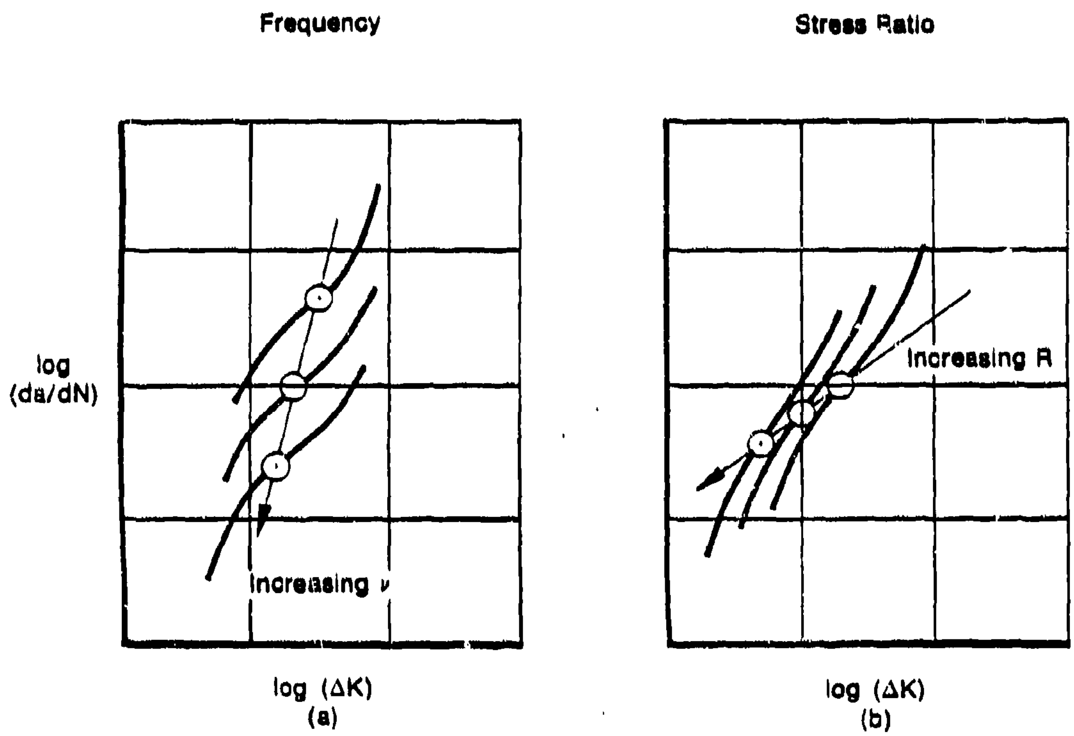

Figure 6. Crack Propagation as Influenced by Test Parameters

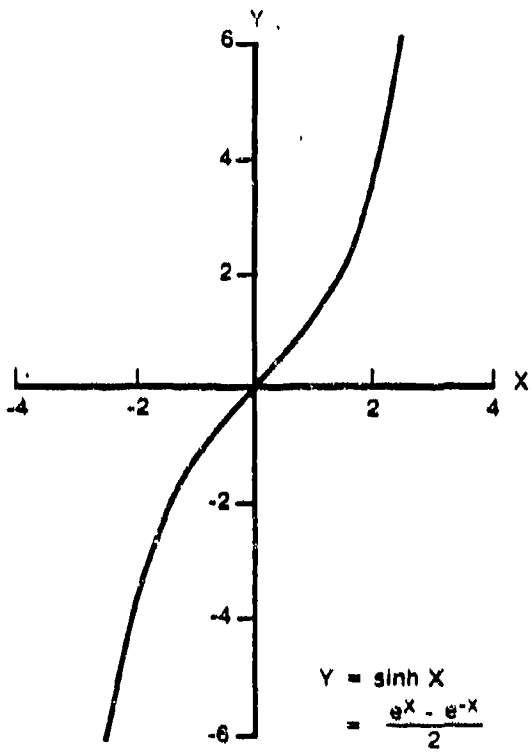

Figure 7. The Hyperbolic Sine Function

variations of da/dN versus ΔK data. The SINH modeling equation will now be derived, starting with the definition of the sinh function.

$$y = \sinh x = \frac{e^{x}-e^{-x}}{2} \tag{5}$$

The inflection point for sinh, which normally falls at (0,0) can be shifted by the addition of two constants C_3 and C_4 as follows:

$$(y - C_4) = \sinh(x + C_3) \tag{6}$$

Here, C_3 locates the horizontal position and C_4 locates the vertical position of the inflection point. The curve can be stretched vertically by the addition of a constant C_1 and horizontally by the addition of a constant C_2 such that the equation now reads

$$\frac{(y - C_4)}{C_1} = \sinh(C_2(x + C_3), \tag{7}$$

and can be written as

$$y = C_1 \sinh(C_2(x + C_3) + C_4 \tag{8}$$

Substituting log(da/dN) for y, and log(ΔK) for x, the final PW SINH equation becomes

$$\log(da/dN) = C_1 \sinh(C_2(\log(\Delta K) + C_3) + C_4 \tag{9}$$

When this equation is applied to predict crack growth rates, the following assumptions are made:

C_1 = material constant (0.5 for IN718)

$C_2 = f_2(\nu, t_H, R)$

$C_3 = f_3(\nu, t_H, R)$

$C_4 = f_4(\nu, t_H, R)$.

The essence of the SINH model is to find these functional relationships which relate the SINH equation constants to the test parameters. In this work, these functional relationships were all assumed to be linear on log-log plots. Also, it was assumed that the changes due to ν, t_H, and R are independent of each other, and therefore their effects can be accounted for by linear superposition. This suggests that the values of the constants C_2, C_3, and C_4 which account for variations in each of the test parameters are obtained from

$$C_j = C_{j\,baseline} + \Delta C_j \qquad j = 2,3,4 \tag{10}$$

where

$$\Delta C_j = (\partial C_j/\partial \nu)\Delta \nu + (\partial C_j/\partial t_H)\Delta t_H + (\partial C_j/\partial R)\Delta R \tag{11}$$

and the Δ's refer to differences from the baseline values. Specifically, when j = 2, the assumed form becomes

$$C_2 = C_{2\ baseline} + b_1 \log \nu + b_2 \log(t_H+1) + b_3 \log((1-R)/.9) \tag{12}$$

where the last three terms on the right-hand side account for the changes in C_2 caused by the variation of each test parameter from the baseline condition. The divisor (.9) in the last term forces the term to vanish at the baseline value of R. The addition of unity to t_H in the next-to-last term is a slight non-linearity which solves the mathematical difficulty when t_H equals zero.

The constants b_1, b_2, and b_3 appearing in the last three terms in Equation 12 were determined as follows. Referring back to Figure 3, it can be seen that the test matrix was designed to allow for the segregation of the ν, t_H, and R dependencies. There are two different values of each test parameter. This forms three unique groups of two data sets. Each of these groups contains the baseline data set and another data set in which only one of the three parameters has been varied. Consider the group of data sets where ν is varied. In this case, Equation 12 reduces to the first two terms, because the R and t_H terms vanish at the baseline values. The procedure used to find b_1 was to: (1) fit the best SINH curve to the baseline data set, (2) fit the best SINH curve to the set in which ν is varied, and (3) fit a straight line between the two values of C_2 found in steps (1) and (2). The slope of this straight line is b_1. The same process was repeated for the other data-set groups to obtain the last two terms in Equation 12. Expressions for the remaining SINH constants, C_3 and C_4, were obtained in the same manner. Pratt and Whitney's SINH computer program was used to automate this process. In PW's SINH computer program (5), an iterative scheme using least-squares regression is used to find the SINH equation constants for each data set starting with initial guesses supplied by the user. The program also supplies the straight-line fits to constants derived from groups of data sets in which only one test parameter is varied.

MSE Model

The Modified Sigmoidal Equation (MSE) model was developed by General Electric (6), and is given by the following expression:

$$da/dN = e^{B'}(\Delta K/\Delta K_i)^P[\ln(\Delta K/\Delta K^*)]^Q[\ln(\Delta K_c/\Delta K)]^D \qquad (13)$$

Here

ΔK_i = ΔK at the inflection point of the curve

ΔK^* = the vertical asymptote at crack growth threshold

ΔK_c = the vertical asymptote at maximum crack growth rate

Q = lower shaping coefficient

D = upper shaping coefficient

and

$$D = -[Q^{1/2}\ln(\Delta K_i/\Delta K_c)/\ln(\Delta K_i/\Delta K^*)]^2 \qquad (14)$$

$$P = (da/dN_i)' - Q/\ln(\Delta K_i/\Delta K^*) + D/\ln(\Delta K_c/\Delta K_i) \qquad (15)$$

$$B' = \ln(da/dN_i) - Q\ln[\ln(\Delta K_i/\Delta K^*)] - D\ln[\ln(\Delta K_c/\Delta K_i)] \qquad (16)$$

where

da/dN_i = the crack growth rate at the inflection point

$(da/dN_i)'$ = the slope at the inflection point.

Figure 8 shows the MSE equation plotted and indicates the manner in which the coefficients in the MSE equation affect the da/dN versus ΔK curve (6). The coefficients Q and D control the sharpness of the transition from the inflection point to the asymptotes. Decreasing the absolute value of these constants, causes a sharper transition. When D is set equal to minus Q, a symmetric curve results. B' is the distance by which the inflection point is displaced from a da/dN value of one.

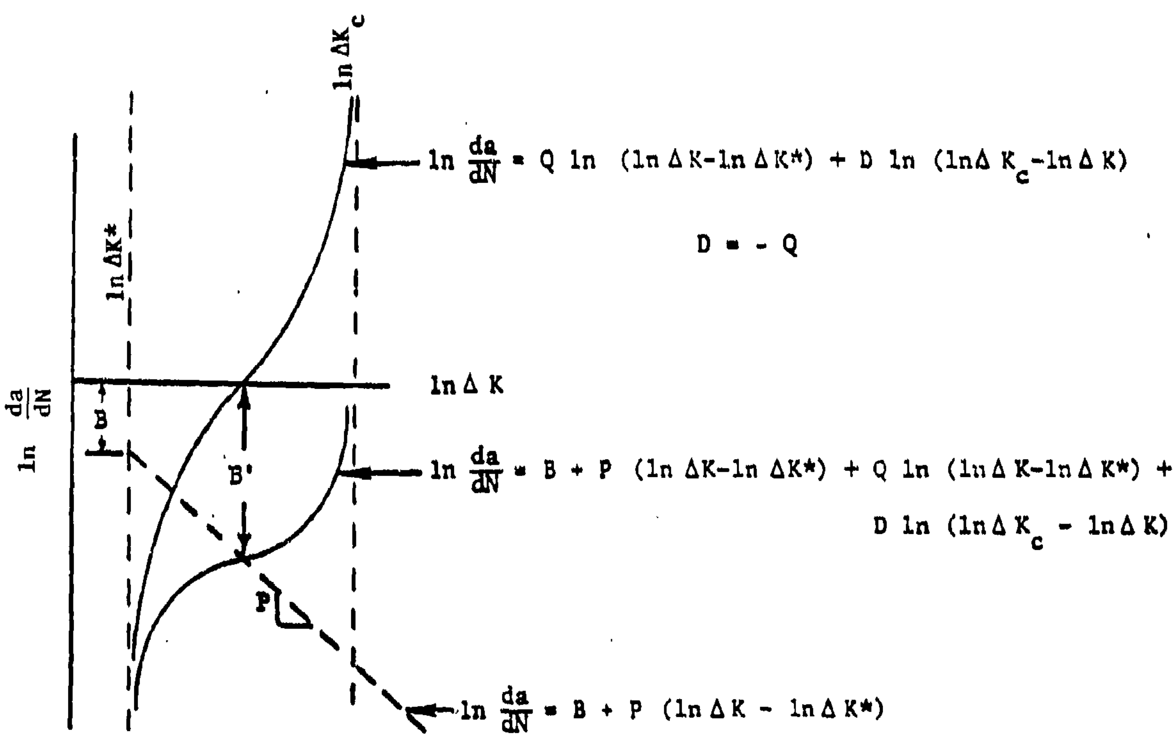

Figure 8. The Effect of the MSE Coefficients on the Sigmoidal Curve (From GE Report (6))

The unprimed B in the figure controls the vertical motion of the whole curve. P controls the rotation of the curve in the vicinity of the inflection point.

A comparison of the SINH and MSE models reveals that there are analogies between the two sets of coefficients employed by each model. Coefficients ΔK_i, da/dN_i, $(da/dN_i)'$, ΔK_c, ΔK^*, and Q are analogous to the constants C_1–C_4 in the SINH model. Note that the constants, ΔK_i and da/dN_i, are related directly to the two SINH constants, C_3 and C_4 by the following:

$$C_3 = -\log(\Delta K_i) \tag{17}$$

and

$$C_4 = \log(da/dN_i) \tag{18}$$

As it was done with the SINH model, expressions were derived relating these six constants to the test parameters. The procedure used to determine the SINH constants was also followed in determining the MSE constants. However, since GE's MSE model is not developed to the point of a production code, any regression analysis needed was performed by hand calculations. In fact, as mentioned earlier, the GE MSE model was specifically developed for the alloy AF115, and has not been previously applied to IN718. The General Electric investigators (6) had access to a large data set, and thereby were able to include some higher order dependencies, i.e. terms involving products of functions of the test parameters. The data set used in this investigation was limited by design. Therefore, the linear forms used for the SINH model were also applied to the MSE model. One of the goals of this investigation is to determine whether the use of linear functional forms is adequate. The assumed forms are given as follows:

$$\Delta K_c = d_1 \tag{19}$$

$$\log(\Delta K^*) = \log(\Delta K^*)_{base} + d_2 \log\nu + d_3 \log(t_H+1) \tag{20}$$

$$\log(\Delta K_i) = \log(\Delta K_i)_{base} + d_4 \log(1-R) + d_5 \log\nu + d_6 \log(t_H+1) \tag{21}$$

$$\log(da/dN_i) = \log(da/dN_i)_{base} + d_7 \log(1-R) + d_8 \log\nu + d_9 \log(t_H+1) \tag{22}$$

$$(da/dN_i)' = (da/dN_i)'_{base} + d_{10} \log(1-R) + d_{11} \log\nu + d_{12} \log(t_H+1) \tag{23}$$

$$Q = d_{13} \tag{24}$$

where d_1 through d_{12} are constants determined by linear regression, while d_{13} is determined graphically via an iterative process. There are only two data curves used to resolve a change due to varying a particular test parameter in Equations 19-24. Therefore, the linear regression approach reduces to solving a set of simultaneous equations. For example, in Equation 22, the set of simultaneous equations is a three by three set. The value of da/dN_i is known for the baseline data set and for the three data sets where ν, R, and t_H are varied. These values can be substituted into Equation 22 along with the appropriate values of the test parameters for each data set. The result is three equations in the three unknowns d_7, d_8, and d_9.

The following comments should be made concerning these assumed functional forms: (1) The upper asymptote, ΔK_c, was assumed to be a constant for simplicity and because the experimental data did not extend into this region. This does not over-restrict the shape of the curve, because if Q is not equal to minus D, the bottom half can act independently of the top half. (2) An examination of the experimental data revealed that ΔK^* is only a function of ν and t_H and not R. (3) The slope of the curve at the inflection point, $(da/dN_i)'$, was obtained visually from data plots. The points determined using the SINH computer program to be the inflection points for each data set, were also used for the MSE model. Therefore, the inflection points of curves produced from both models coincide. (4) The lower shaping coefficient, Q, was assumed to be a constant, since it was found graphically via an iterative process that adequate MSE fits could be obtained for all of the experimental data sets with a constant Q. The first attempt to model Q required the use of an expression similar to that given in Equation 23. However, this resulted in an expression which gave unreasonable values of Q for values of the test parameters corresponding to the proof tests, i.e., negative Q's. It was concluded that Q was sensitive to change near the baseline, but was relatively insensitive to values of the test parameters away from the baseline. Therefore, the value of Q found to best represent the baseline condition was also used for the remaining data sets. (5) The motivation for assuming MSE equations of a form analogous to that used for the SINH model, was to determine whether they are valid for either model. They are general equations which could be applied to either a small or a large data set. The objective was to produce functional relationships which do not rely on ad hoc relations suggested by the data itself, but remain valid for any material exhibiting similar fracture toughness characteristics.

IV. Results and Discussion

Experimental Data

All of the data obtained from the experimental program are given in numerical form in Appendix A. The data are grouped according to specimen numbers assigned at the time of testing. The four data sets used for developing the SINH and MSE models are given first. Their specimen numbers are 83264D (baseline data set, R=.1, ν=1 Hz, t_H=0 sec), 83266G (R=.1, ν=.01 Hz, t_H=0 sec), 83270B (R=.5, ν=1 Hz, t_H=0 sec), and 83270 (R=.1, ν=1 Hz, t_H=50 sec). The following two data sets were obtained from the proof tests. These specimens were used to check the predictions of the models developed from the first four data sets. The specimen numbers are 83288 (first proof test, R=.5, ν=.01 Hz, t_H=50 sec), and 83289 (second proof test, R=.25, ν=1 Hz, t_H=10 sec). Finally, there are two groups of constant ΔK data provided from the archives of the Air Force Materials Laboratory taken from tests performed prior to this thesis effort. The first of these sets is for R=.1, t_H=0 sec, and various frequencies at ΔK=22.745 Ksi $\sqrt{\text{inches}}$ and ΔK=36.4 Ksi$\sqrt{\text{inches}}$. The second of these two sets is for R=.1, ν=1 Hz, and various hold times at the same two ΔK's. These two data sets were used to examine the validity of the linear functional relationships assumed for ν and t_H.

The data used for the development of the SINH and MSE models are plotted in Figures 9-12 and also in Figures 13-16. In Figures 9-12, the dashed lines are the SINH-model fits to the data sets, while in Figures 13-16 the dashed lines represent the MSE fits to the data. The large solid squares in Figures 9-12 identify the locations of the inflection

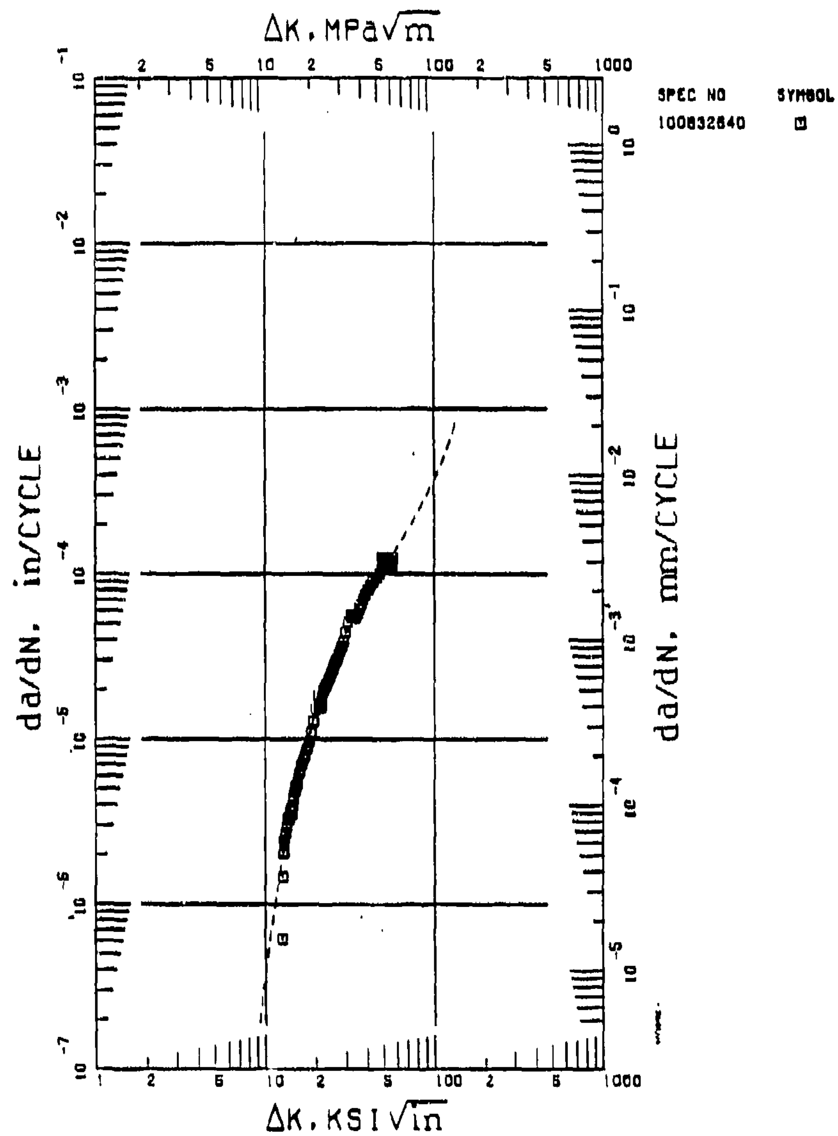

Figure 9. da/dN Versus ΔK, R=.1, ν=1 Hz, t_H=0 sec. SINH Fit Superimposed (Dashed Line)

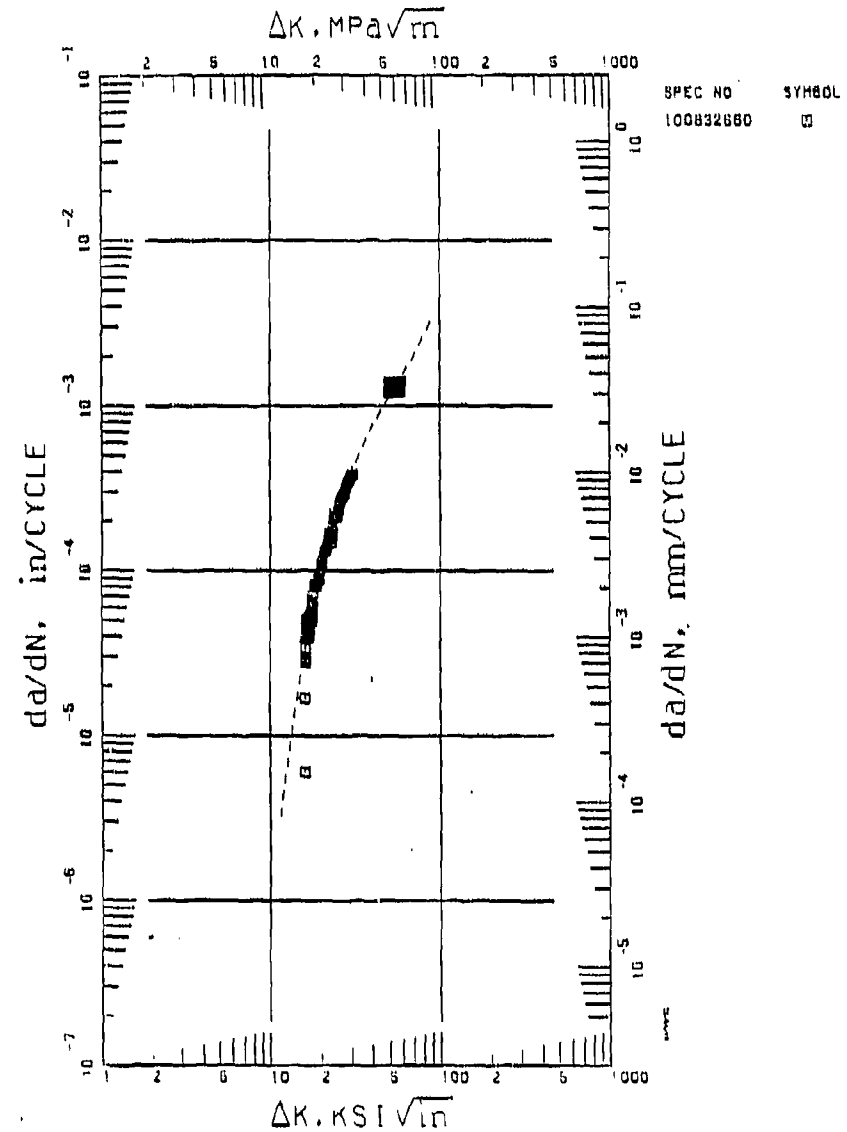

Figure 10. da/dN Versus ΔK, R=.1, ν=.01 Hz, t_H=0 sec. SINH Fit Superimposed (Dashed Line)

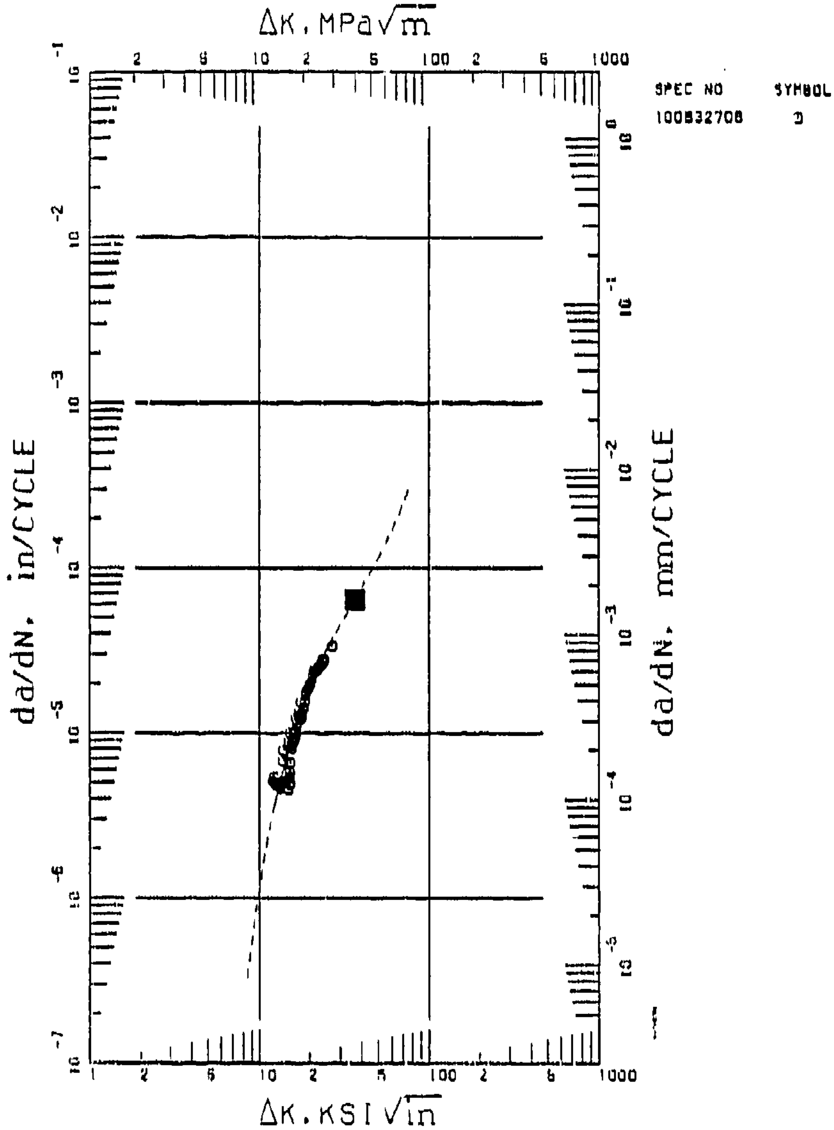

Figure 11. da/dN Versus ΔK, R=.5, ν=1 Hz, t_H=0 sec.
SINH Fit Superimposed (Dashed Line)

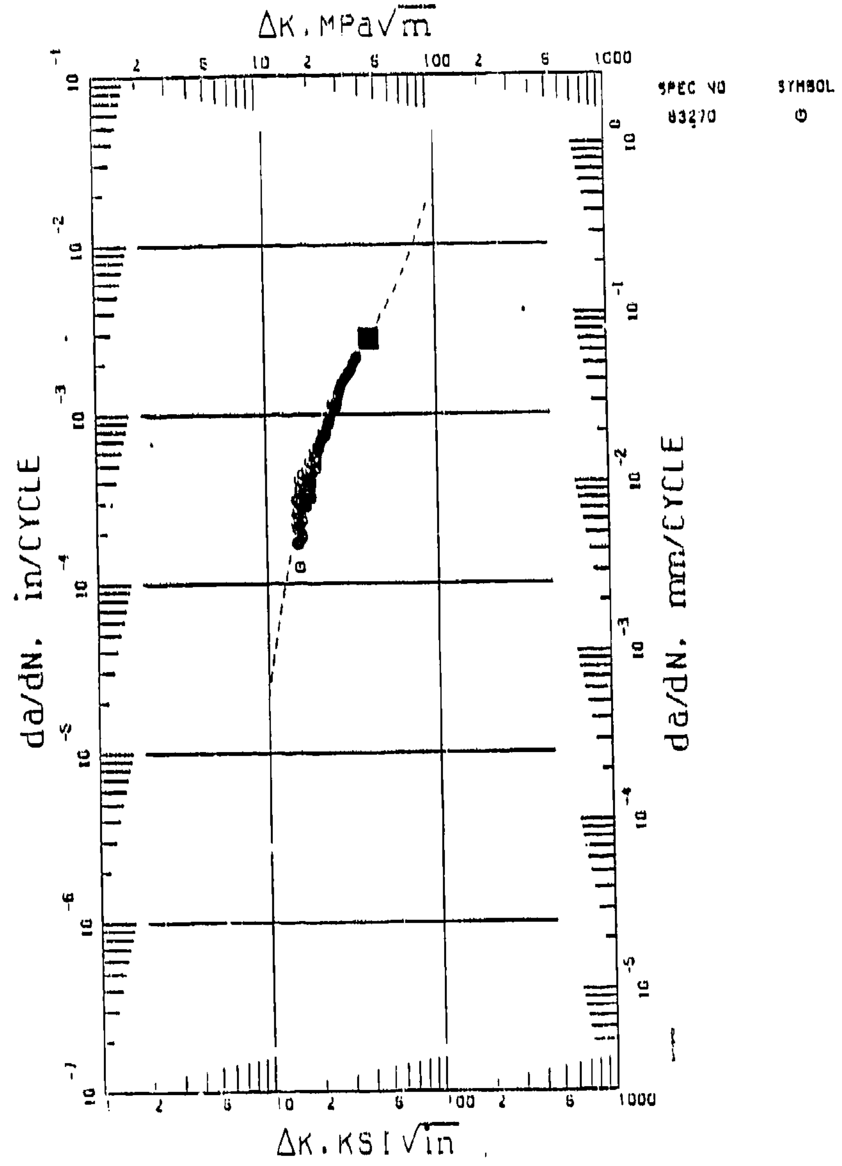

Figure 12. da/dN Versus ΔK, R=.1, ν=1 Hz, t_H=50 sec.
SINH Fit Superimposed (Dashed Line)

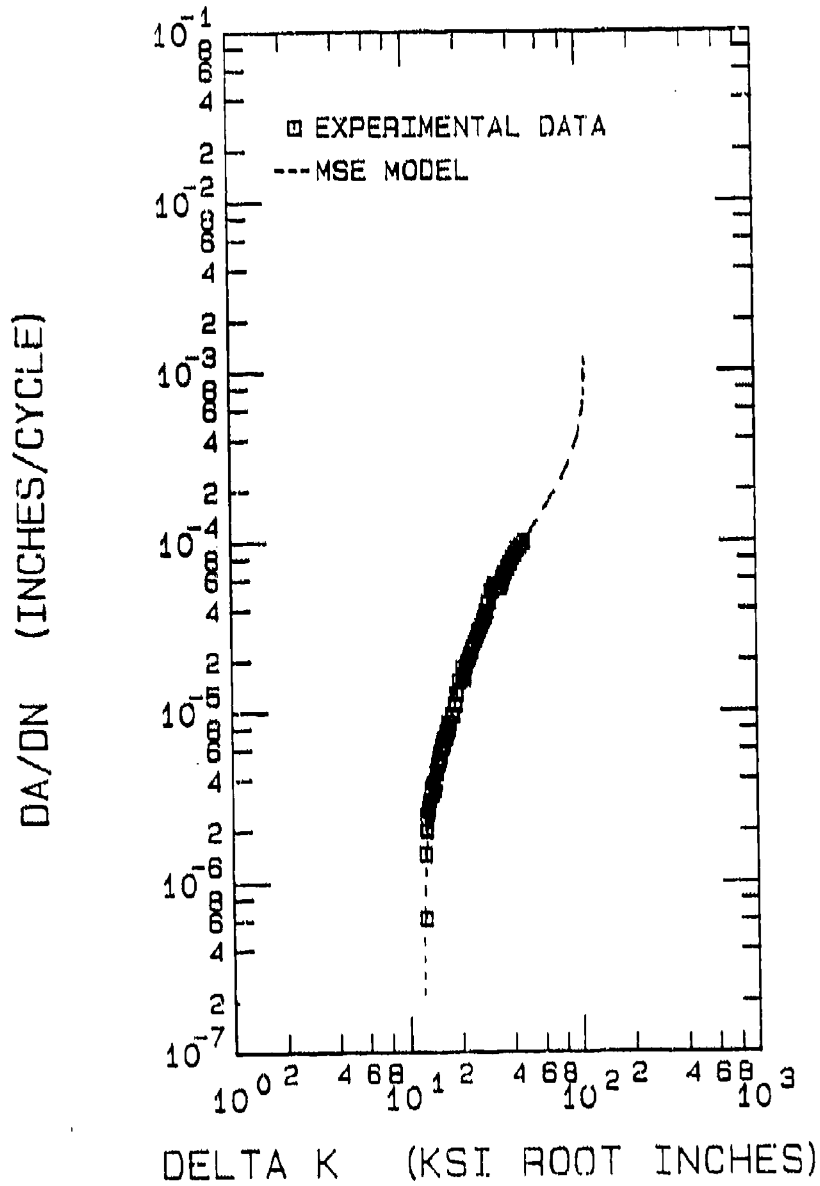

Figure 13. da/dN Versus ΔK, R=.1, ν=1 Hz, t_H=0 sec. MSE Fit Superimposed

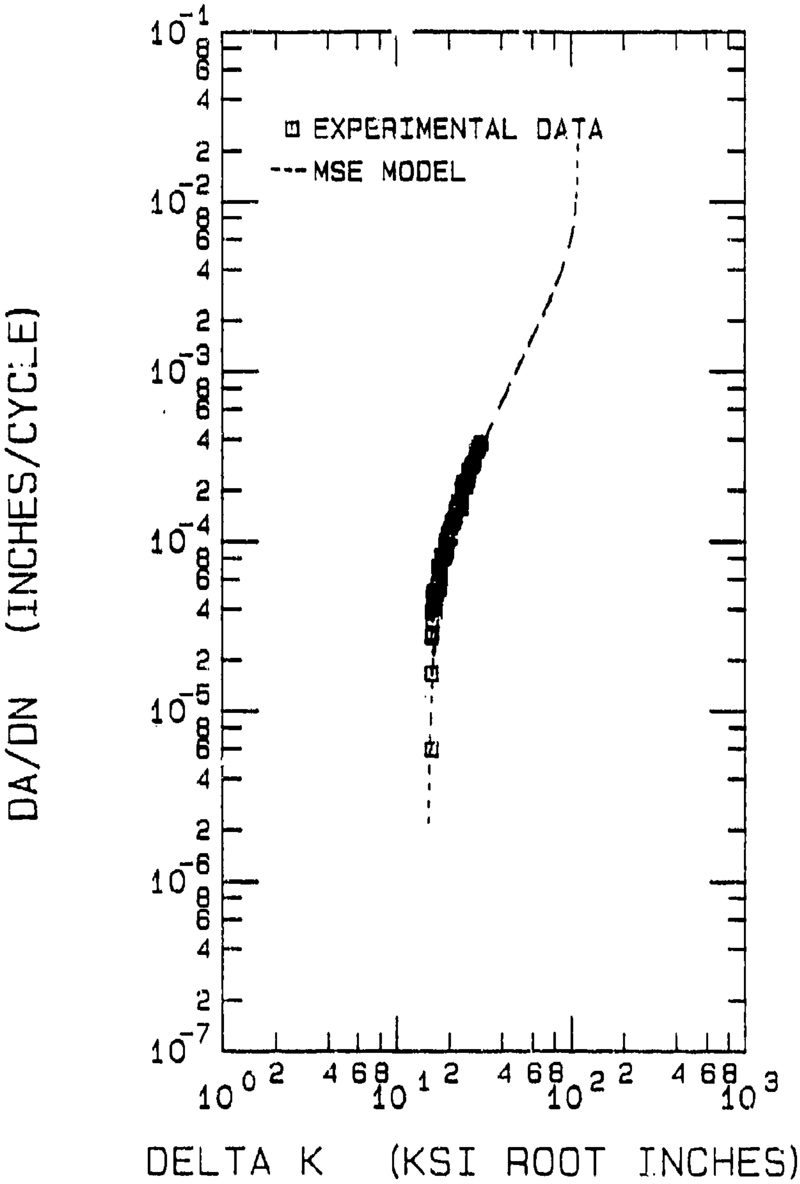

Figure 14. da/dN Versus ΔK, R=.1, ν=.01 Hz, t_H=0 sec. MSE Fit Superimposed

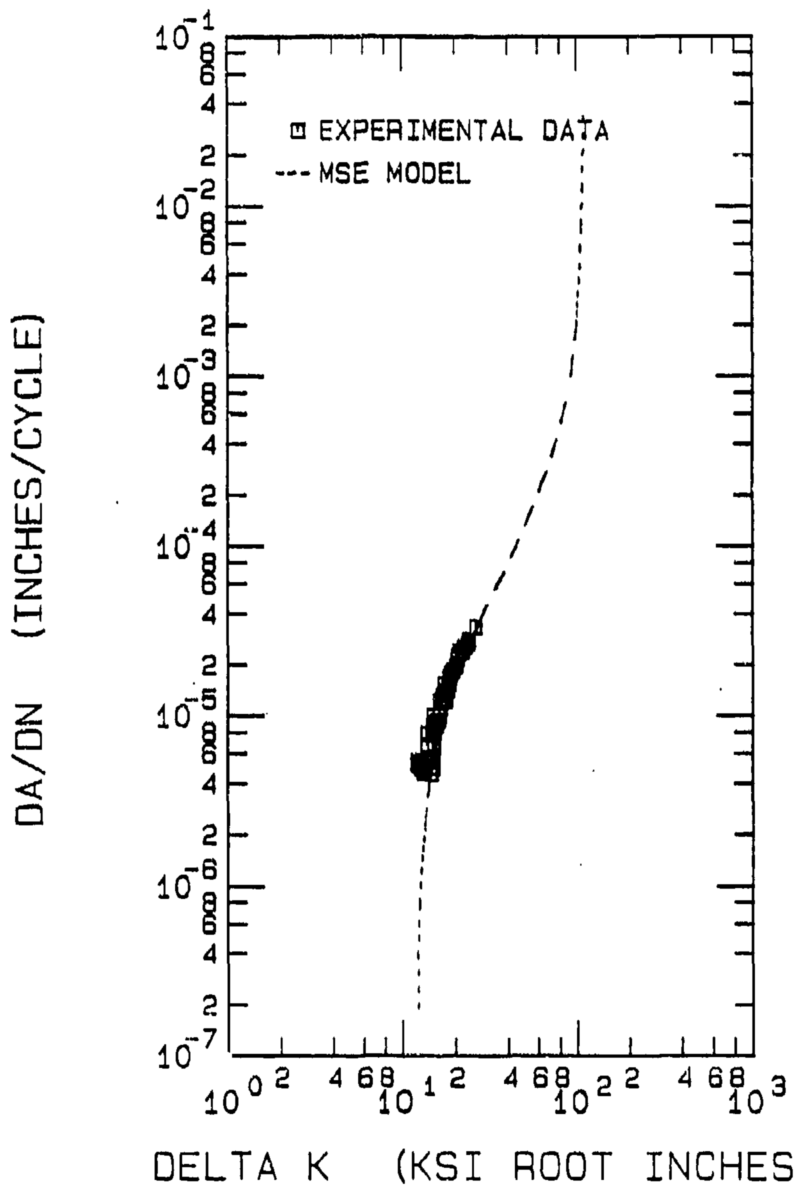

Figure 15. da/dN Versus ΔK, R=.5, ν=1 Hz, t_H=0 sec. MSE Fit Superimposed

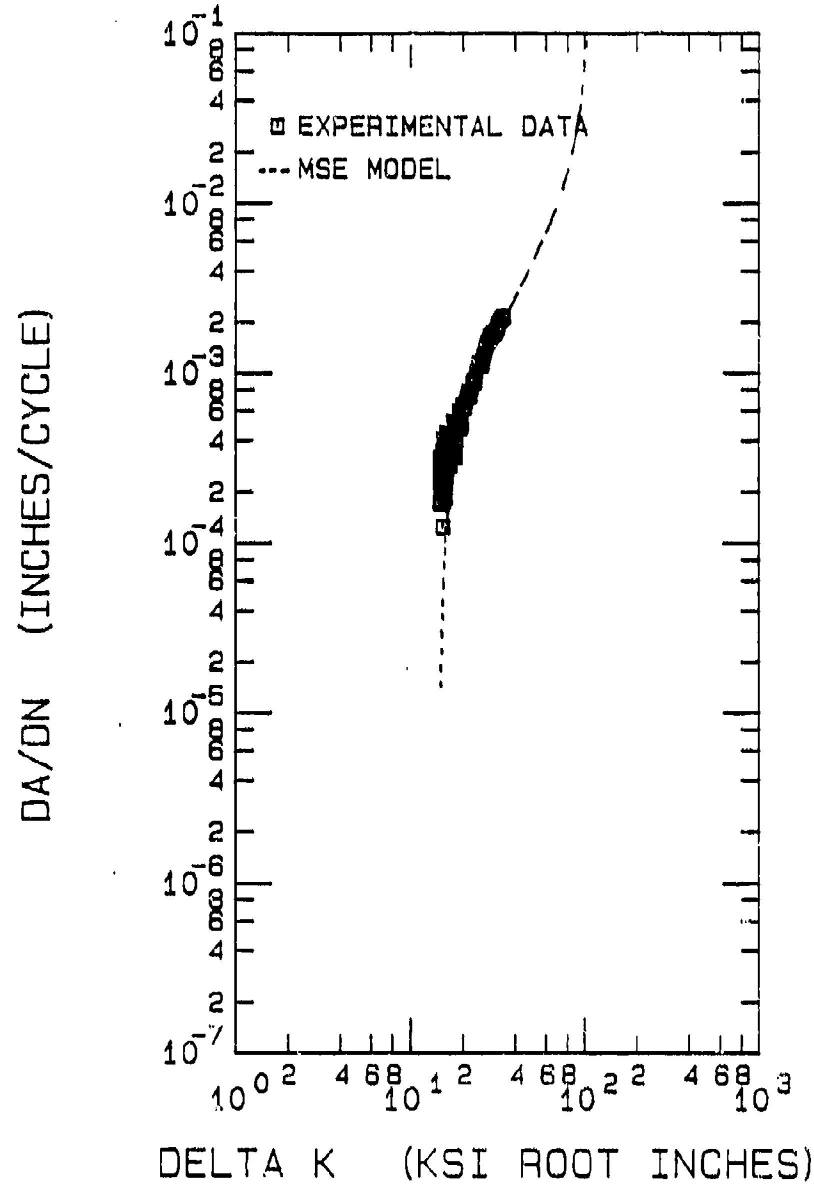

Figure 16. da/dN Versus ΔK, R=.1, ν=1 Hz, t_H=50 sec. MSE Fit Superimposed

points calculated iteratively by PW's SINH program starting with user supplied guesses. It should be noted that the final location of the inflection point depends upon the user's initial guess. This point is discussed in detail in (4).

SINH and MSE Predictions

The reader will recall the procedure described in Section III regarding the segregation and characterization of the changes in the SINH (or MSE) constants due to changes in the test parameters R, ν, and t_H. This procedure consists of grouping experimental data sets in which the values of all the test parameters are the same except for one. Equations are then developed which allow for linear interpolation between the model constants obtained for each data set in a group. After the effects on the constants due to changes in each of the test parameters are isolated and characterized, they are superimposed to form a single equation for each model constant. Figures 17-19 illustrate how this procedure was executed for the SINH model. Figure 17 shows the change in the position of the inflection point due to a change in R, while Figures 18 and 19 show the changes due to changes in ν and t_H respectively. In these figures, the solid lines drawn through the inflection points represent the associated linear fits. The dashed lines are the model fits to each data set. In each of the Figures 17-19, only one test parameter is varied. Similar lines could be drawn for the MSE fits. In fact, they would be the same lines because the same inflection points were chosen for the SINH and MSE curves for each data set, even though the shape of the curves is slightly different.

Using the procedures outlined in Section III, the following expressions were derived representing appropriate interpolative models for the SINH and the MSE equations:

<u>SINH Interpolative Model</u>

$$\log(da/dN) = C_1 \sinh(C_2(\log(\Delta K) + C_3) + C_4 \tag{25}$$

where

$$C_1 = .5 \tag{26}$$

$$C_2 = 3.197 - 1.1675\log[(1-R)/.9] - .1505\log\nu + .2053\log(t_H+1) \tag{27}$$

$$C_3 = -1.721 - .6243\log[(1-R)/.9] + .00717\log\nu + .0677\log(t_H+1) \tag{28}$$

$$C_4 = -3.935 + 1.0131\log[(1-R0/.9] - .523\log\nu + .8127\log(t_H+1) \tag{29}$$

and

<u>MSE Interpolative Model</u>

$$da/dN = e^{B'}(\Delta K/\Delta K_i)^P[\ln(\Delta K/\Delta K^*)]^Q[\ln(\Delta K_c/\Delta K)]^D \tag{30}$$

where

$$\Delta K_c = 109.9 \tag{31}$$

$$\Delta K^* = 10^{[1.08918 - .04846\log\nu + .05675\log(t_H+1)]} \tag{32}$$

$$\Delta K_i = 10^{[1.721 + .6243\log((1-R)/.9) - .00717\log\nu - .0677\log(t_H+1)]} \tag{33}$$

$$Q = 1.0 \tag{34}$$

and

$$da/dN_i = 10^{[-3.935 + 1.0131\log((1-R)/.9) - .523\log\nu + .8127\log(t_H+1)]} \tag{35}$$

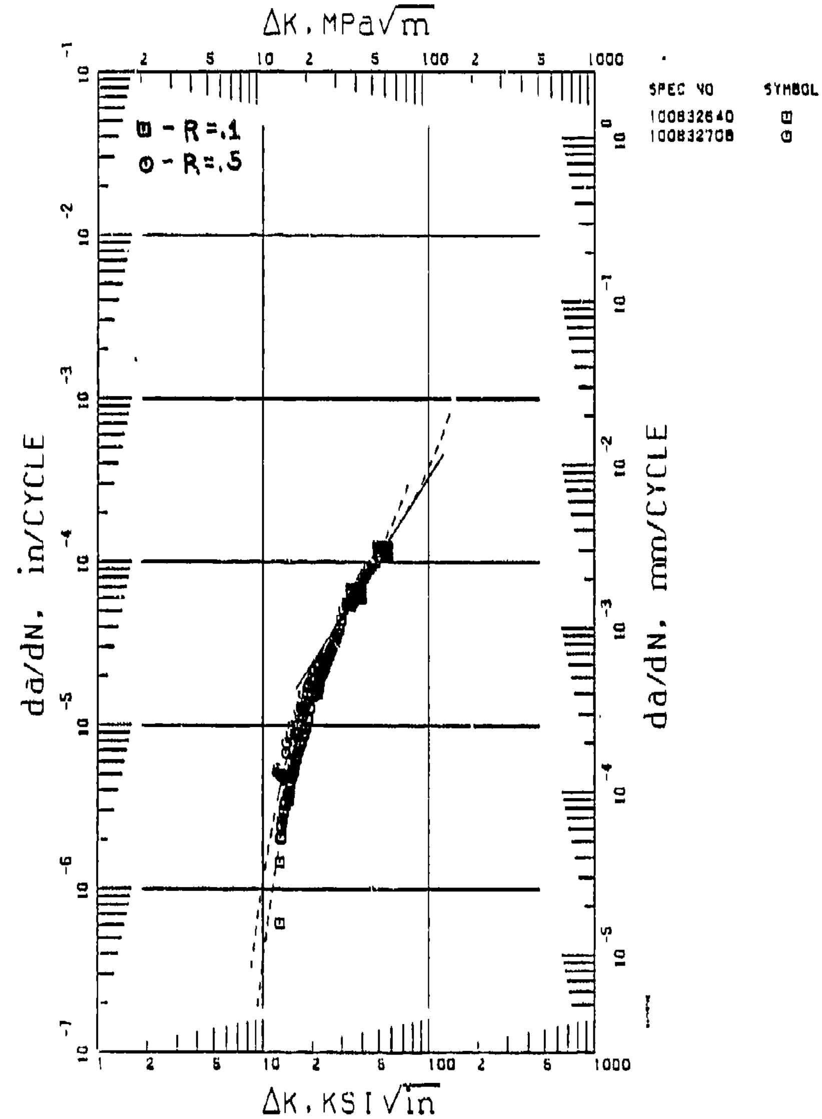

Figure 17. Effect of Stress Ratio (R) on the Location of the da/dN versus ΔK Inflection Point (R=.1 to R=.5) (Dashed lines indicate SINH model fits. Solid line is linear fit through inflection points.)

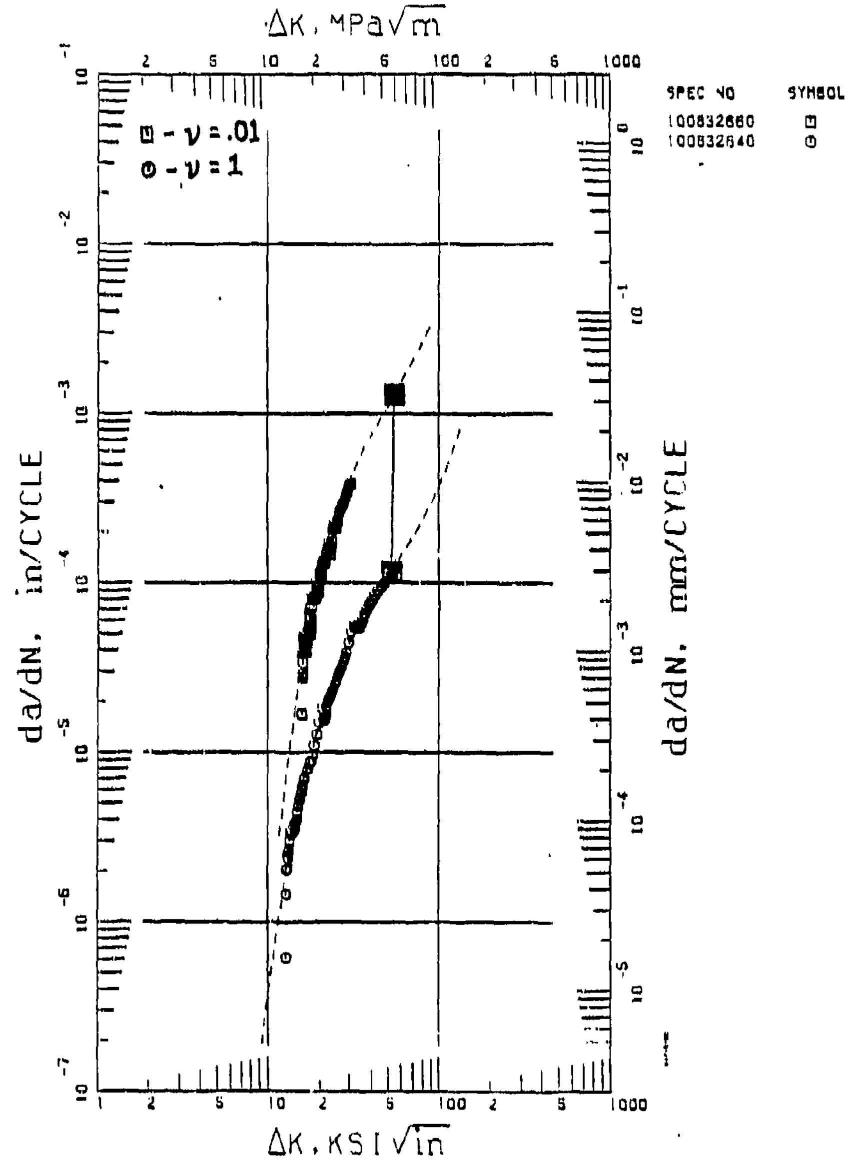

Figure 18. Effect of Frequency (ν) on the Location of the da/dN versus ΔK Inflection Point (ν=1 Hz to ν=.01 Hz) (Dashed lines indicate SINH model fits. Solid line is linear fit through inflection points.)

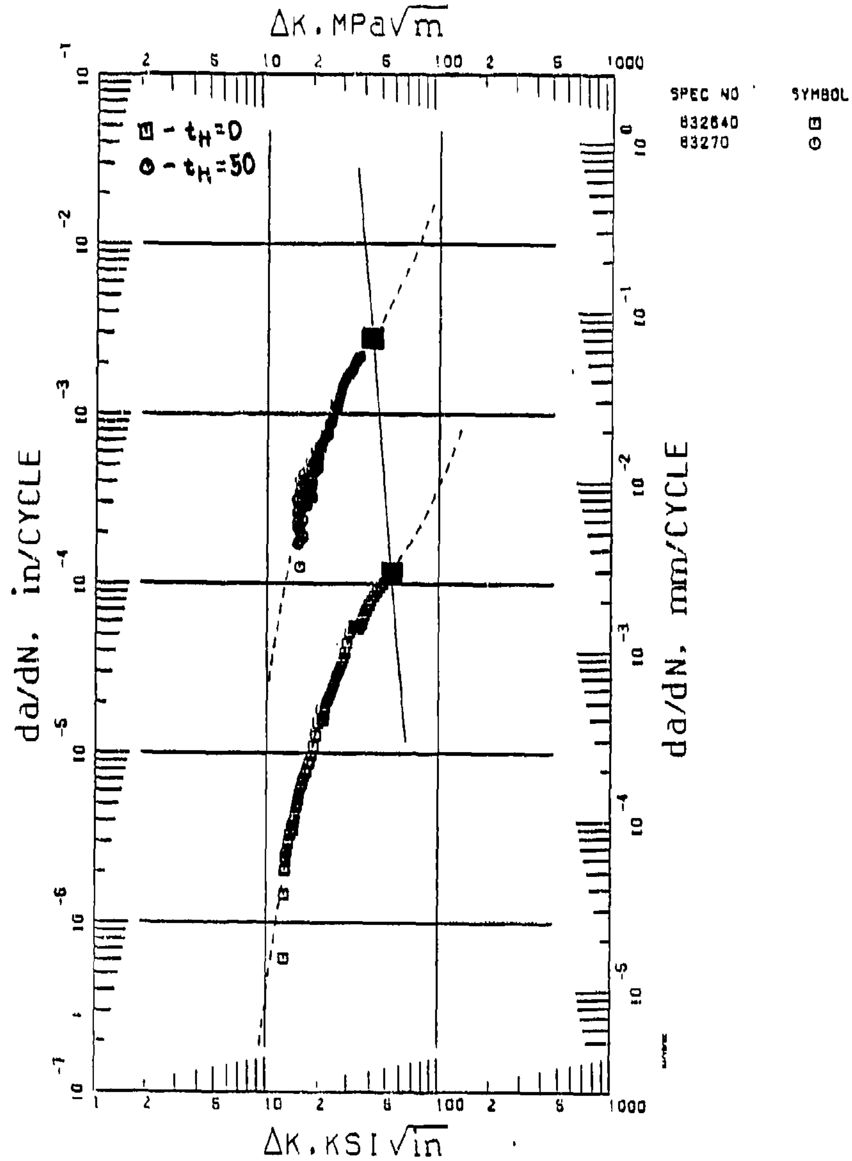

Figure 19. Effect of Hold Time (t_H) on the Location of the da/dN versus ΔK Inflection Point (t_H=0 sec to t_H=50 sec) (Dashed lines indicate SINH model fits. Solid line is linear fit through inflection points.)

$$D = -\,[Q^{1/2}\ln(\Delta K_i/\Delta K_c)/\ln(\Delta K_i/\Delta K^*)]^2 \qquad (36)$$

$$P = (da/dN_i)' - Q/\ln(\Delta K_i/\Delta K^*) + D/\ln(\Delta K_c/\Delta K_i) \qquad (37)$$

$$B' = \ln(da/dN_i) - Q\ln[\ln(\Delta K_i/\Delta K^*)] - D\ln[\ln(\Delta K_c/\Delta K_i)]. \qquad (38)$$

$$(da/dN_i)' = 1.7 - 1.8451\log[(1-R)/.9] - .2185\log \;+ .1956\log(t_H+1) \qquad (39)$$

Note that Equations 25 and 30 were previously given as Equations 9 and 13 respectively. Also, Equations 36, 37, and 38 are the same as 14, 15, and 16. In the above expressions, C_3 has the units of log(Ksi $\sqrt{\text{in.}}$), C_4 has the units of log(inches/cycle), C_1, C_2, $(da/dN_i)'$, Q, D, and P are dimensionless, ΔK_c, ΔK_i, and ΔK^* have the units of Ksi $\sqrt{\text{in.}}$, and B' has the units of ln(inches/cycle). Both the SINH and the MSE Interpolative Models were programed in standard FORTRAN, and the resulting interactive computer codes appear in Appendix B and in Appendix C, respectively. These similar codes calculate the constants for the corresponding model at T= 1200 F, when R, ν, and t_H are given as input. They also give da/dN values for requested ΔK values. They are based on a limited data set, and they are given here to show how the models were applied.

Discussion

A few comments are in order concerning the SINH and MSE interpolative models as developed.

In Equations 27, 28, 29, 33, 35, and 39, the .9 divisor in the R-change terms has been included as an offset used to force the R-change term to vanish when R is at its baseline value.

Figures 13-16 show the initial MSE fits to the four data sets from which the models were constructed. These fits were obtained by hand calculations. However, the initial SINH fits, shown in Figures 9-12, were obtained with the aid of Pratt and Whitney's SINH computer program which uses an iterative regression scheme. Even with this aid, a great deal of user judgement is required in order to obtain a good fit. The initial SINH fits were obtained first. Then, the MSE constants which control the inflection point were given analogous values found from the initial SINH fits. With the inflection point identified in the MSE model, and using a constant lower-shaping coefficient, Q, and assuming that the two asymptotes are correct, the only quantity that can improve the initial MSE fits is the constant $(da/dN_i)'$. Recall that this constant controls the slope of the curve at the inflection point. All of these initial MSE slope constants were computed by hand, by visually measuring the slopes from data plots. In order to get the best possible MSE fits, it was necessary to adjust both Q and $(da/dN_i)'$ simultaneously. Using a larger slope at the inflection point requires the use of a smaller Q, in order to keep the same curvature in the lower portion of the curve.

The interpolative models were compared against two proof tests. The data from these proof tests were not used in the formulation of the models, and were taken at arbitrary values of the test parameters. The results obtained from Proof Test One ($R=.5$, $\nu=.01$ Hz, $t_H=50$ sec) are shown in Figure 20, while those from Proof Test Two ($R=.25$, $\nu=1$ Hz, $t_H=10$ sec) are shown in Figure 21. Let us first examine Proof Test One (Figure 20). Both the SINH and the MSE models matched closely in their predictions, with the MSE predicting a steeper slope. SINH appears to

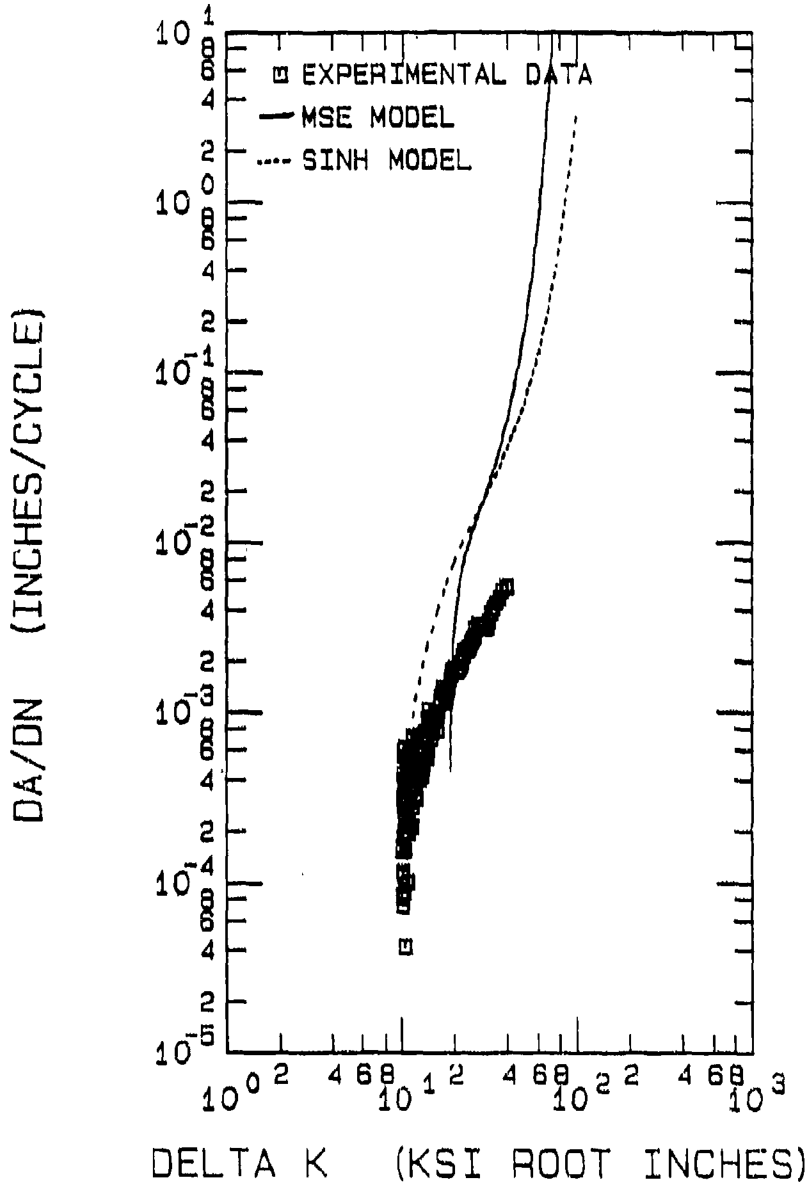

Figure 20. Comparison of Predicted and Experimental da/dN Proof Test One (R=.5, ν=.01 Hz, t_H=50 sec)

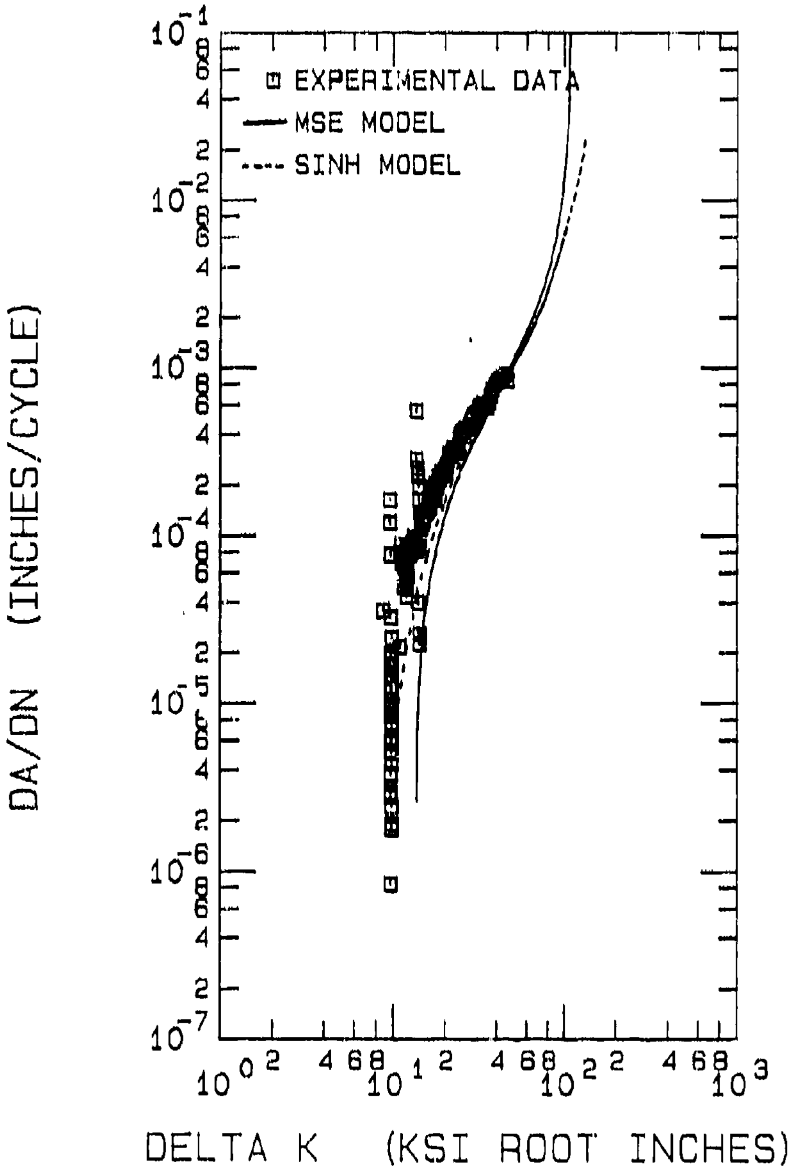

Figure 21. Comparison of Predicted and Experimental da/dN Proof Test Two (R=.25, ν=1 Hz, t_H=10 sec)

predict a more correct threshold ΔK (SINH does not have a true threshold), but both seemed to predict da/dN values greater by a factor of about four than the experimental results. Also, the slope of both predicted curves seemed to be too steep.

Consider next the results of the Second Proof Test (Figure 21). Here, the two predictions match each other closely except for the natural differences between the two equations. Also, the threshold value of ΔK was predicted more closely than in the First Proof Test. The overall accuracy of the prediction was much closer, say, within a factor of one to two. This better accuracy may be attributed to the fact that the values of the test parameters for these data are closer to the baseline values. Also, only two test parameters were changed from the baseline values, while all three were changed in Proof Test One. The limited accuracy of these two predictive comparisons is not surprising considering the variability inherent in fatigue crack-growth data. ASTM standard E 647-81 (7) states that da/dN data may vary by a factor of two. Considering that only two data points were used to establish each linear relationship in a system given to those kind of variabilities, it is not surprising that the predictions could be in error by a factor of four.

Another type of comparison was made using the constant ΔK data given in the last two pages of Appendix A. Figures 22 and 23 compare da/dN for various hold times at ΔK=32.75 Ksi $\sqrt{in.}$ and ΔK=22.724 Ksi $\sqrt{in.}$, respectively. This data was taken from a different batch of specimens, which explains the offset of approximately a factor of two. Figures 24 and 25 compare da/dN for various frequencies also at ΔK=32.75 Ksi$\sqrt{in.}$ and ΔK=22.745 Ksi $\sqrt{in.}$. Figures 22-25 represent an attempt to

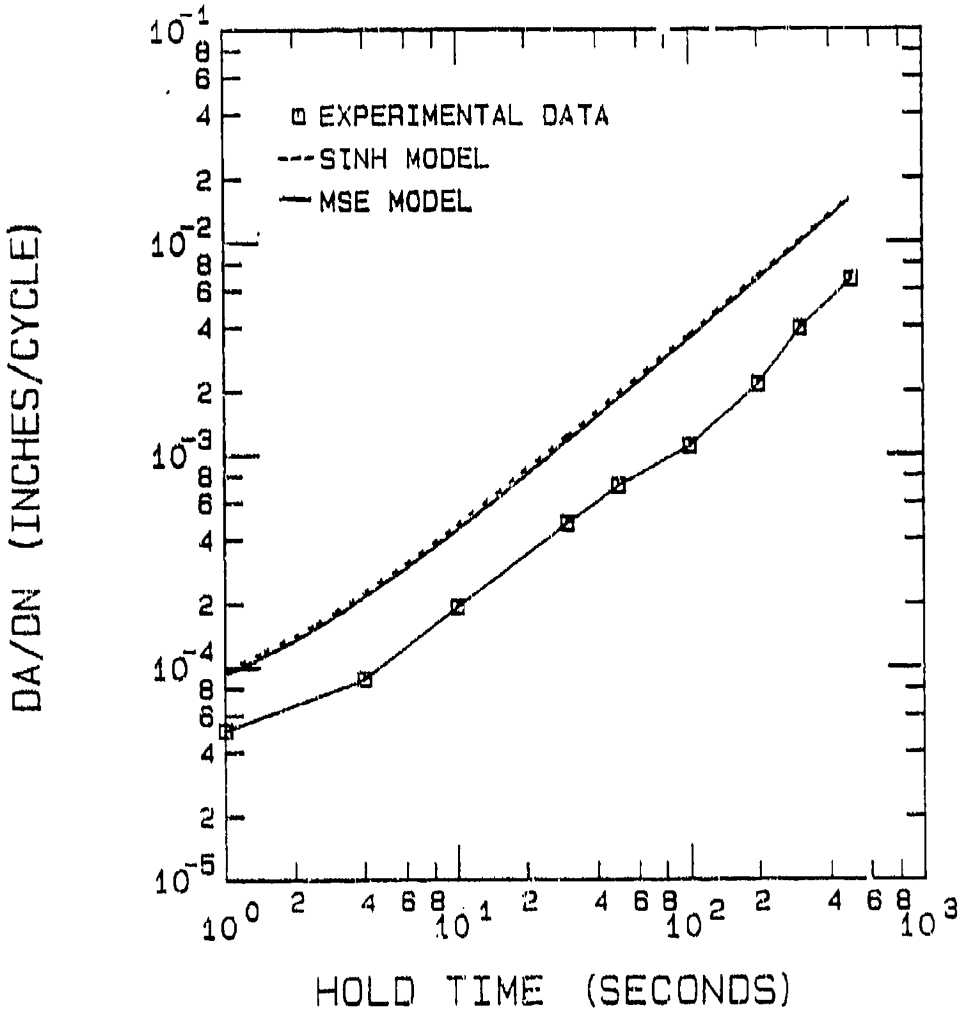

Figure 22. Comparison of Predicted and Experimental da/dN Data for ΔK=32.75 Ksi root in (R=.1, ν=1 Hz, Variable t_H)

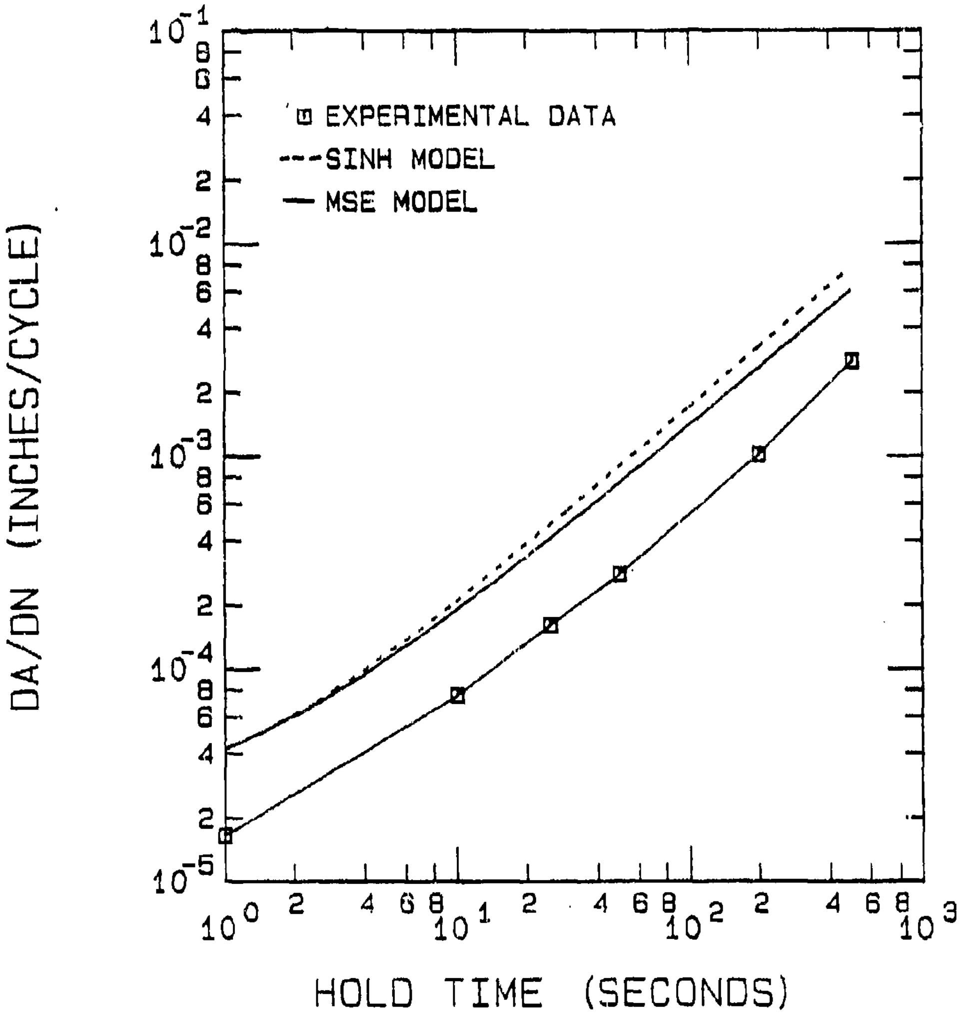

Figure 23. Comparison of Predicted and Experimental da/dN Data for ΔK=22.745 Ksi root in (R=.1, ν=1 Hz, Variable t_H)

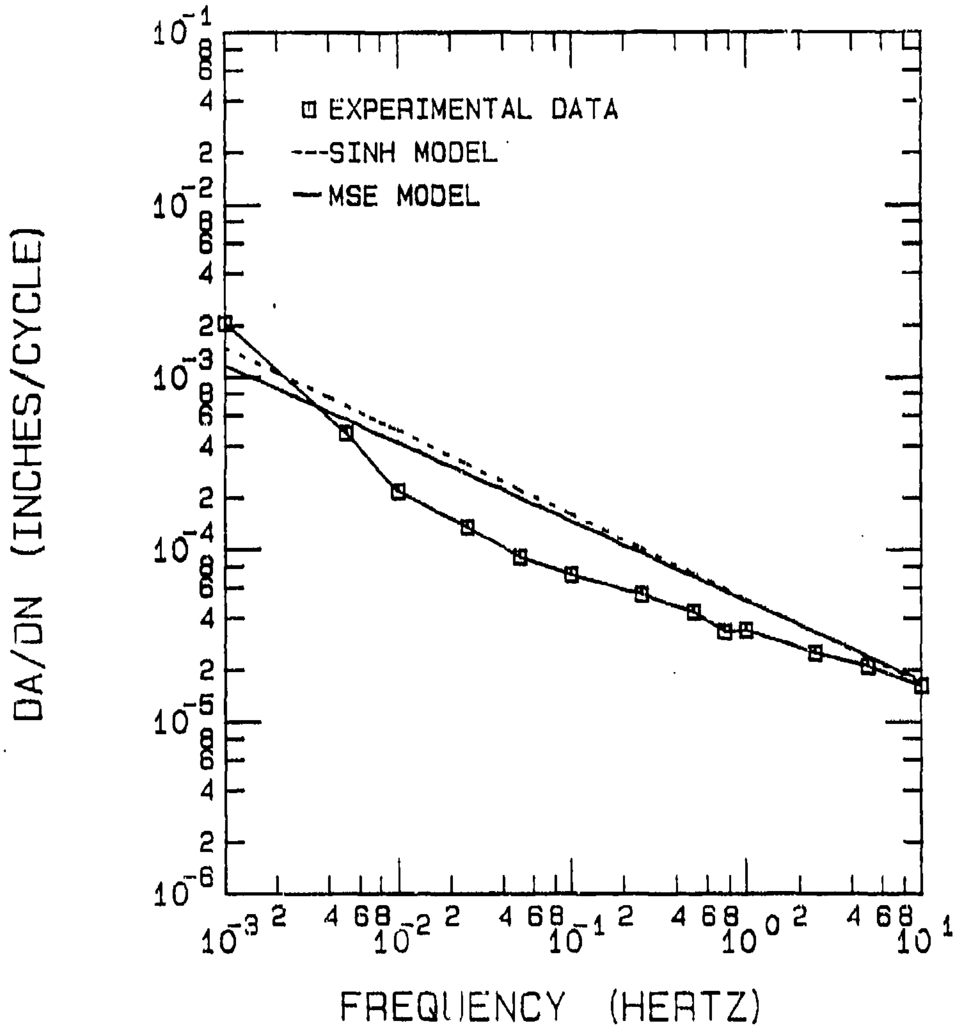

Figure 24. Comparison of Predicted and Experimental da/dN Data for ΔK=32.75 Ksi root in (R=.1, t_H=0 sec, variable ν)

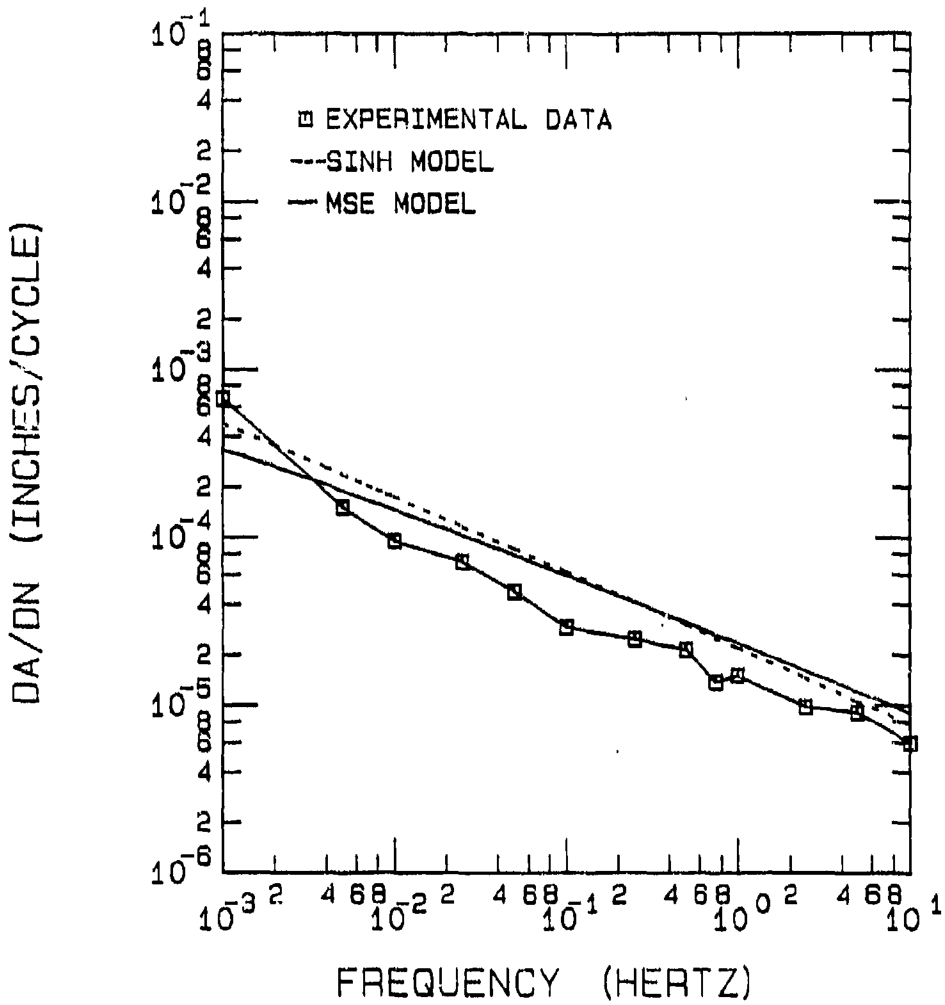

Figure 25. Comparison of Predicted and Experimental da/dN Data for ΔK=22.745 Ksi root in (R=.1, t_H=0 sec, variable ν)

examine the validity of assuming linear functional relationships (on log-log plots) relating the test parameters to the SINH and MSE constants. In these plots only one test parameter was varied at a time, with the other test parameters kept at baseline values. Figures 22 and 23 show da/dN versus hold time (t_H) for two different ΔK's. Notice that the SINH and MSE curves are slightly non-linear. As mentioned earlier, this is because $\log(t_H+1)$ was assumed as a functional relationship rather than the $\log(t_H)$ as was suggested in (3). Assuming this form, takes care of the mathematical difficulty encountered at $t_H=0$, and seems to match the form of the experimental data better than a straight line would. This is true at least for IN718. In Figures 25 and 26, da/dN versus frequency (ν) is plotted for two different ΔK's. Note that in both figures the experimental data shows a definite upward turn at the lower frequencies. This cannot be modeled by a straight line. However, considering the amount of variability of the experimental data, a straight line seems adequate for a wide range of ν.

V. Conclusions and Recommendations

Form of Crack Growth Rate Equation

This exercise has shown that it makes little difference which form of equation is used to model fatigue crack growth rate data. Both the Hyperbolic Sine and the Modified Sigmoidal Equation have sufficient flexibility to model da/dN data. Both forms give essentially the same answers when the same functional forms are used to relate the test parameters to the equation constants. The MSE equation offers a little more flexibility in that a non-symmetric curve can be modeled as well as a symmetric curve. Also, the MSE equation has the advantage of exhibiting true asymptotic behavior at the threshold and high crack-growth-rate regions of the da/dN versus ΔK curve.

It has been shown that the same functional relationships used in the SINH model can be applied to the MSE model. Therefore, the same iterative regression techniques employed in Pratt and Whitney's SINH computer program could be applied to the MSE model. Thus, the MSE model could be automated, making it a more usable tool.

Relating Constants to Test Parameters

The method used to relate the SINH or MSE constants to the test parameters is what makes either one of them a model and not just an equation. Certainly, if every possible combination of test parameters were tested, then relationships could be developed to model exactly any condition of interest. However, if all possible tests were performed, the model would no longer be needed. The reason for the model is to reduce the number of tests necessary to characterize the crack growth behavior of the material in question. Even if all possible tests were performed, there would still be the possibility of a two hundred percent error from test to test performed under the same conditions. The question of whether linear (on log-log plots) relationships are adequate to relate the model constants to the test parameters cannot be fully explored with such a small data set as was used here. However, any higher order interactions would probably yield changes in da/dN which are much smaller than the 200 percent variability of the data. Therefore, the question is probably moot. If linear (on log-log plots) relationships are employed to construct SINH or MSE models, the models are adequate for a large range of ΔK. This is true, providing the region of model use is not too far from the baseline condition. The reader will recall that it was assumed that changes in da/dN due to variations in each of the test parameters are independent and can be linearly superimposed. The model would be more accurate near the baseline condition because any inaccuracies introduced by this linear superposition would be minimized when summing small individual changes. A larger number of tests, with replication of as many tests as possible is desirable in order to develop any real confidence in models developed from a particular data base.

Future work should investigate the type of functional relationships that are appropriate, using a much larger data base than the one generated for this investigation. Based on the examination of the results obtained from the two proof tests, it would seem that linear superposition of slopes and inflection-point coordinates might not be valid. On the other hand, with such a small data base, small errors in the linear interpolations for each test parameter would be magnified when their effects are superimposed. This again, points out the need for a larger data base.

Appendix A: Experimental Data

Specimen 83264D (Baseline Data Set, $R=.1$, $\nu=1$ Hz, $t_H=0$ sec)

ΔK	da/dN
12.599000	0.61370000E-06
12.625400	0.14596000E-05
12.678200	0.20198000E-05
12.758300	0.24883000E-05
12.832000	0.24217000E-05
12.885600	0.20665000E-05
12.927500	0.23672000E-05
12.992100	0.25621000E-05
13.064000	0.27196000E-05
13.154000	0.26661000E-05
13.226800	0.29269000E-05
13.305100	0.30447000E-05
13.372400	0.30093000E-05
13.467000	0.33797000E-05
13.582600	0.32559000E-05
13.680800	0.34933000E-05
13.764500	0.32903000E-05
13.852800	0.36374000E-05
13.966500	0.37328000E-05
14.093000	0.37527000E-05
14.225800	0.38424000E-05
14.325900	0.34922000E-05
14.418700	0.38277000E-05
14.526000	0.39996000E-05
14.676100	0.44189000E-05
15.000900	0.48992000E-05
15.159300	0.52055000E-05
15.324800	0.52990000E-05
15.516800	0.57335000E-05
15.734300	0.61535000E-05
15.965300	0.63996000E-05
16.207400	0.68929000E-05
16.470300	0.70933000E-05
16.766000	0.75638000E-05
17.071700	0.79354000E-05
17.407400	0.85925000E-05
18.186200	0.96055000E-05
18.639300	0.10954700E-04
19.184300	0.12741300E-04
19.858400	0.15042900E-04
20.732800	0.18056700E-04
20.774600	0.15779500E-04
21.016600	0.15861000E-04
21.220400	0.15572400E-04
21.457900	0.16617300E-04
21.745400	0.18522000E-04
22.053800	0.19684600E-04
22.735200	0.21055500E-04
23.097300	0.21737800E-04
23.469500	0.22763300E-04
23.890700	0.23882600E-04
24.347400	0.25173600E-04
24.855100	0.26543600E-04
25.391000	0.28223600E-04
25.867700	0.29463300E-04
26.373600	0.30638900E-04
26.938600	0.32263300E-04
27.534500	0.34285000E-04
28.200500	0.36271200E-04
28.924700	0.38646000E-04
29.758100	0.44244000E-04
30.759800	0.51129800E-04
32.005300	0.56401500E-04
32.076300	0.54173100E-04
32.815000	0.55940800E-04
33.522900	0.55535300E-04
34.207900	0.53684900E-04
34.964900	0.57184900E-04
35.816500	0.61267600E-04
36.762700	0.65133700E-04
37.800800	0.69625800E-04
38.973500	0.74743900E-04
40.311900	0.79684900E-04
41.823100	0.84677000E-04
43.530800	0.90114000E-04
45.486000	0.95054900E-04
47.642200	0.10019670E-03

Specimen 83266G (R=.1, ν=.01 Hz, t_H=0 sec)

ΔK	da/dN	ΔK	da/dN
15.793400	0.59646000E-05	19.133300	0.10171240E-03
15.804300	0.16774000E-04	19.239800	0.99380000E-04
15.826100	0.27583000E-04	19.414400	0.87531300E-04
15.858000	0.38392400E-04	19.488100	0.89881700E-04
15.918000	0.47370000E-04	19.580900	0.10008640E-03
15.976300	0.46582600E-04	19.687400	0.10799580E-03
16.000800	0.28948800E-04	19.817500	0.11166120E-03
16.026300	0.33642100E-04	19.948500	0.11499980E-03
16.060000	0.40909000E-04	20.056800	0.10773600E-03
16.143700	0.50078600E-04	20.165000	0.10433440E-03
16.212800	0.48873900E-04	20.268700	0.10581470E-03
16.272900	0.44527500E-04	20.375200	0.11861790E-03
16.298300	0.39444800E-04	20.518900	0.12694860E-03
16.327500	0.39862100E-04	20.669100	0.13047000E-03
16.365700	0.38914500E-04	20.830100	0.13185010E-03
16.413900	0.41507800E-04	20.981100	0.13275560E-03
16.465700	0.48637700E-04	21.121200	0.13344070E-03
16.513100	0.51602300E-04	21.265900	0.13142490E-03
16.567600	0.40893600E-04	21.436000	0.13746430E-03
16.609500	0.40783400E-04	21.602500	0.14221800E-03
16.649500	0.47822700E-04	21.777200	0.14862180E-03
16.701400	0.45873900E-04	21.950100	0.15641310E-03
16.747800	0.39123200E-04	22.153000	0.15969000E-03
16.785100	0.43031400E-04	22.364900	0.17043270E-03
16.848800	0.46992000E-04	22.602400	0.16697210E-03
16.877000	0.50397500E-04	22.819900	0.16228000E-03
17.013400	0.54121900E-04	23.161000	0.15706270E-03
17.079900	0.53224300E-04	23.305700	0.16149970E-03
17.121700	0.53765540E-03	23.424900	0.17466890E-03
17.226300	0.55905400E-04	23.608700	0.20541300E-03
17.302800	0.65523500E-04	23.818800	0.21221220E-03
17.403800	0.70507700E-04	24.049900	0.22533030E-03
17.479300	0.62114000E-04	24.266500	0.21643260E-03
17.536600	0.56098300E-04	24.489400	0.21513340E-03
17.600300	0.52549000E-04	24.672200	0.21090510E-03
17.700400	0.53602300E-04	24.884200	0.21170040E-03
17.775000	0.53066800E-04	25.100800	0.22623940E-03
17.830500	0.60535300E-04	25.345500	0.23283420E-03
17.893200	0.72212500E-04	25.603900	0.24760190E-03
17.997900	0.81842400E-04	25.874100	0.26016480E-03
18.107900	0.82322700E-04	26.164300	0.26456250E-03
18.215300	0.79275400E-04	26.481800	0.27666480E-03
18.326300	0.80759700E-04	26.795700	0.27952700E-03
18.390000	0.80094300E-04	27.127800	0.28825930E-03
18.479200	0.81177000E-04	27.470800	0.29139310E-03
18.596500	0.83456500E-04	27.818400	0.30559780E-03
18.715700	0.80614000E-04	28.629900	0.33940880E-03
18.796700	0.82696700E-04	29.099400	0.34902690E-03
18.867600	0.83161300E-04	29.584300	0.36035360E-03
18.921300	0.84527400E-04	30.091100	0.37663310E-03

Specimen 83270B (R=.5, ν=1 Hz, t_H=0 sec)

ΔK	da/dN
26.770200	0.33575100E-04
23.921600	0.28068100E-04
23.688700	0.27067300E-04
23.078200	0.25862200E-04
22.503200	0.25311400E-04
21.977400	0.24122400E-04
21.257700	0.24105100E-04
21.255900	0.23480700E-04
20.763700	0.22769600E-04
20.418000	0.21503500E-04
19.954900	0.19712600E-04
19.455400	0.18627100E-04
19.004100	0.17825600E-04
18.708400	0.16949600E-04
18.616500	0.15456700E-04
18.188900	0.14153100E-04
17.590300	0.15377500E-04
17.743100	0.13073600E-04
17.661200	0.12305100E-04
17.430100	0.13105500E-04
17.173600	0.13359400E-04
16.975200	0.12725900E-04
16.431200	0.12188600E-04
16.579500	0.11153500E-04
16.302900	0.10068900E-04
16.168200	0.93669000E-05
15.782500	0.92354000E-05
15.879800	0.92480000E-05
15.754300	0.87858000E-05
15.542300	0.89842000E-05
15.396700	0.80098000E-05
15.211100	0.66224000E-05
15.101000	0.57909000E-05
15.153800	0.49209000E-05
14.946400	0.49953000E-05
15.001900	0.53894000E-05
14.728000	0.45468000E-05
14.842600	0.82976000E-05
15.145600	0.10003500E-04
14.879900	0.88311000E-05
13.872800	0.78366000E-05
13.823700	0.67594000E-05
13.657200	0.54952000E-05
13.174000	0.49055000E-05
13.073100	0.47142000E-05
12.982100	0.45890000E-05
12.846500	0.49453000E-05
12.554500	0.50342000E-05
12.684600	0.48464000E-05
12.543600	0.48563000E-05
12.079500	0.51524000E-05
12.210600	0.54268000E-05

Specimen 83270 (R=.1, ν=1 Hz, t_H=50 sec)

ΔK	da/dN	ΔK	da/dN
14.753500	0.31376710E-03	16.811500	0.41039290E-03
14.790800	0.25961760E-03	16.866100	0.35951500E-03
14.809900	0.22712950E-03	16.907900	0.28622780E-03
14.835400	0.17298000E-03	16.931600	0.32201120E-03
14.843600	0.29995220E-03	16.973400	0.34307810E-03
14.882700	0.30562930E-03	17.027100	0.41322750E-03
14.917200	0.21157040E-03	17.099000	0.42204640E-03
14.959100	0.25876720E-03	17.168100	0.42090470E-03
14.991800	0.31683790E-03	17.228200	0.42271570E-03
15.037300	0.27470810E-03	17.321900	0.43492040E-03
15.052800	0.17003120E-03	17.392800	0.38186540E-03
15.090100	0.17757440E-03	17.456500	0.40452680E-03
15.109200	0.25813200E-03	17.506600	0.42354250E-03
15.152900	0.27185380E-03	17.566600	0.38299530E-03
15.216600	0.31475920E-03	17.622100	0.36844810E-03
15.263900	0.34575130E-03	17.672100	0.32557810E-03
15.315700	0.29609390E-03	17.729500	0.38605040E-03
15.339400	0.17795240E-03	17.768600	0.35463710E-03
15.358500	0.19896810E-03	17.890500	0.51704620E-03
15.382200	0.12462180E-03	17.984200	0.47909350E-03
15.390300	0.21940900E-03	18.071600	0.45873920E-03
15.407600	0.25294040E-03	18.131600	0.38506620E-03
15.457700	0.35510560E-03	18.173500	0.37372370E-03
15.517700	0.40681020E-03	18.215300	0.32190490E-03
15.581400	0.36412920E-03	18.247100	0.40873930E-03
15.643300	0.37520000E-03	18.334500	0.50743990E-03
15.666900	0.28497970E-03	18.420900	0.51023520E-03
15.704200	0.28662150E-03	18.504600	0.51822730E-03
15.734300	0.31705450E-03	18.583800	0.46578650E-03
15.786100	0.30724350E-03	18.649300	0.50759740E-03
15.834300	0.34959380E-03	18.792100	0.48326680E-03
15.883500	0.28182230E-03	18.870400	0.49897540E-03
15.912600	0.30527100E-03	18.938600	0.55271540E-03
15.954400	0.27892860E-03	19.030500	0.59952640E-03
15.993500	0.19253110E-03	19.119700	0.56747920E-03
16.024500	0.18644060E-03	19.227000	0.58948700E-03
16.029900	0.18772000E-03	19.327100	0.57779410E-03
16.067200	0.29848760E-03	19.410800	0.51618010E-03
16.131800	0.40602280E-03	19.470800	0.48027460E-03
16.215500	0.44047160E-03	19.547300	0.50232180E-03
16.279200	0.38465670E-03	19.630100	0.55598310E-03
16.315600	0.38350320E-03	19.722900	0.58472320E-03
16.370200	0.34325130E-03	19.819300	0.63842390E-03
16.398400	0.33034190E-03	19.936700	0.64791210E-03
16.457600	0.34993240E-03	20.041300	0.64499870E-03
16.516700	0.33201510E-03	20.151400	0.64145540E-03
16.558500	0.30278290E-03	20.251500	0.62602240E-03
16.579500	0.29382620E-03	20.353400	0.63366020E-03
16.626800	0.36095600E-03	20.453400	0.63283340E-03
16.668600	0.37718030E-03	20.569900	0.66936870E-03

Specimen 83270 (R=.1, ν=1 Hz, t_H=50 sec)

ΔK	da/dN
21.037500	0.72157340E-03
21.167600	0.72889620E-03
21.294100	0.75157330E-03
21.429700	0.76110080E-03
21.575200	0.78145510E-03
21.710800	0.75358120E-03
21.849100	0.73637650E-03
21.980100	0.76129770E-03
22.114800	0.75007720E-03
22.254900	0.77858110E-03
22.398600	0.82381720E-03
22.563300	0.86696680E-03
22.738000	0.88318720E-03
22.905400	0.88822660E-03
23.090100	0.90176980E-03
23.264800	0.88283290E-03
23.428500	0.89783290E-03
23.611400	0.92484070E-03
23.800600	0.97708470E-03
24.000800	0.10372814E-02
24.478400	0.11515331E-02
24.737700	0.11334100E-02
24.996100	0.11277112E-02
25.470100	0.11022813E-02
25.713100	0.11258639E-02
25.979600	0.11760606E-02
26.267100	0.12541707E-02
26.572800	0.13001549E-02
26.889400	0.13695642E-02
27.246100	0.14414932E-02
27.622700	0.15011781E-02
28.024900	0.15573197E-02
28.445200	0.16019653E-02
28.896500	0.16462172E-02
29.352300	0.16892486E-02
29.856300	0.17250753E-02
30.378600	0.17315713E-02
30.899000	0.17843271E-02
31.455800	0.18458625E-02
32.049000	0.19523583E-02
32.714000	0.20412558E-02
33.479200	0.21142871E-02
34.277100	0.21683028E-02

Specimen 83288 (First Proof Test, R=.5, ν=.01 Hz, t_H=50 sec)

ΔK	da/dN	ΔK	da/dN
10.0516	3.88838E-06	10.9195	2.27606E-04
10.0534	8.14447E-05	10.9796	.0005924
10.0598	.000159	11.056	5.94763E-04
10.0943	8.46061E-05	11.1261	5.05235E-04
10.0989	1.5274E-04	11.177	4.52716E-04
10.0534	1.63189E-04	11.1688	4.14527E-04
10.0852	3.11681E-04	11.2325	3.71373E-04
10.1262	1.86389E-04	11.2598	2.13909E-04
10.1153	7.42676E-05	11.2826	3.73346E-04
10.1025	4.34054E-04	11.3108	4.80944E-04
10.1307	1.15413E-04	11.3481	4.66968E-04
10.1371	3.27425E-04	11.3826	5.28149E-04
10.1662	5.58739E-04	11.4927	5.9055E-04
10.2153	5.91968E-04	11.5528	4.38188E-04
10.2408	1.0937E-04	11.5555	2.78582E-04
10.2363	2.83673E-04	11.5691	2.13885E-04
10.2153	7.32676E-05	11.5746	3.71094E-04
10.2144	2.80799E-04	11.6019	5.3055E-04
10.2736	1.1646E-04	11.6947	7.23306E-04
10.2927	2.30567E-04	11.7802	7.18542E-04
10.259	4.02283E-04	11.8585	6.11889E-04
10.2572	3.53208E-04	11.9149	6.15274E-04
10.2863	5.93503E-04	11.9558	3.73574E-04
10.3491	8.74172E-05	11.9813	3.12035E-04
10.3591	3.64913E-04	12.0104	3.5661E-04
10.3727	3.71133E-04	12.0386	4.2992E-04
10.3318	1.97468E-04	12.0795	5.44605E-04
10.3682	3.42086E-04	12.1423	4.74723E-04
10.4155	2.48755E-04	12.2197	5.27834E-04
10.4701	3.74212E-04	12.2542	5.58188E-04
10.3764	2.86594E-04	12.2897	6.85471E-04
10.41	6.24763E-04	12.3752	5.64802E-04
10.4665	5.95589E-04	12.4353	6.10038E-04
10.5292	5.27873E-04	12.5217	7.08975E-04
10.491	2.01511E-04	12.5818	6.88857E-04
10.5001	4.22086E-05	12.6473	4.0681E-04
10.4892	1.54141E-04	12.6591	5.29369E-04
10.5292	3.11598E-04	12.7464	7.29684E-04
10.5793	4.82007E-04	12.7992	7.36888E-04
10.5975	3.01027E-04	12.9011	6.39841E-04
10.6639	4.27401E-04	12.9748	6.60117E-04
10.6857	3.39507E-04	13.0794	6.09093E-04
10.7039	2.74098E-04	13.0776	4.23306E-04
10.7394	2.14059E-04	13.1095	5.8429E-04
10.7339	3.12889E-04	13.1932	4.66889E-04
10.7703	4.77991E-04	13.265	6.44959E-04
10.8158	5.98424E-04	13.3151	6.69684E-04
10.9004	4.31023E-04	13.4106	7.14408E-04
10.9578	3.00059E-04	13.4725	5.82164E-04
10.9796	1.96527E-04	13.518	7.58818E-04

Specimen 83288 (First Proof Test, $R=.5$, $\nu=.01$ Hz, $t_H=50$ sec)

ΔK	da/dN	ΔK	da/dN
13.7181	6.11062E-04	25.0107	2.60377E-03
13.7854	5.43188E-04	25.4492	.0027085
13.8546	5.4681E-04	25.9123	2.85177E-03
13.8928	6.00904E-04	26.4582	3.10984E-03
13.9237	6.6807E-04	27.1114	3.29621E-03
14.0593	8.97085E-04	27.8338	3.23137E-03
14.1612	9.20471E-04	28.4989	3.10948E-03
14.2913	1.03264E-03	29.1712	3.14496E-03
14.4278	9.42833E-04	29.8345	3.12881E-03
14.5288	7.67951E-04	30.5214	3.19814E-03
14.6061	7.06967E-04	31.3302	3.44704E-03
14.688	7.69526E-04	32.2737	3.86003E-03
14.7626	7.60983E-04	33.3518	4.12716E-03
14.8599	7.72636E-04	34.5646	4.44645E-03
14.9837	8.52518E-04	36.0212	4.76298E-03
15.101	8.38896E-04	37.6252	5.17834E-03
15.1838	8.8492E-04	39.5422	5.49645E-03
15.2839	9.45982E-04		
15.4222	1.01846E-03		
15.5841	1.04437E-03		
15.7379	9.94329E-04		
15.8671	9.37715E-04		
15.9672	7.90628E-04		
16.0518	8.89408E-04		
16.1755	1.02583E-03		
16.3402	1.13244E-03		
16.5203	1.23267E-03		
16.7132	1.29996E-03		
16.9134	1.41551E-03		
17.1172	1.33114E-03		
17.3373	.0013359		
17.563	1.30027E-03		
17.7568	1.24279E-03		
17.9487	1.15331E-03		
18.0943	1.23291E-03		
18.329	1.32106E-03		
18.561	1.38665E-03		
18.8067	1.56035E-03		
19.0978	1.68019E-03		
19.4381	1.76267E-03		
19.7583	1.75098E-03		
20.1468	1.83937E-03		
20.5171	1.76511E-03		
20.8383	1.74874E-03		
21.2104	1.80582E-03		
21.6171	1.86945E-03		
22.0338	1.97078E-03		
22.5023	2.14645E-03		
23.0591	2.28842E-03		
23.646	2.34996E-03		

Specimen 83289 (Second Proof Test, R=.25, ν=1 Hz, t_H=10 sec)

ΔK	da/dN	ΔK	da/dN
9.5666522	0.16375164E-03	11.550948	0.49716435E-04
9.6330684	0.12005881E-03	11.574603	0.64177035E-04
9.6785589	0.76362050E-04	11.610995	0.66799077E-04
9.7040335	0.32670406E-04	11.662854	0.77932913E-04
9.6794687	0.28036164E-05	11.716533	0.77503780E-04
9.6794687	0.29657420E-05	11.753835	0.67680965E-04
9.6785589	0.38258190E-05	11.785679	0.65306954E-04
9.6894766	0.58436889E-05	11.814793	0.58877833E-04
9.6894766	0.83944712E-05	11.849366	0.69960488E-04
9.6949354	0.52149501E-05	11.893946	0.66799077E-04
9.6931158	0.83649437E-06	11.940347	0.55724296E-04
9.6894766	0.16207054E-04	11.963092	0.56110122E-04
9.7049433	0.99232082E-05	11.993116	0.43354243E-04
9.7122218	0.14924773E-04	12.009492	0.47873919E-04
9.7140414	0.16815320E-04	12.028598	0.49775490E-04
9.7276886	0.19088938E-04	12.067720	0.60389641E-04
9.7331475	0.18692482E-04	12.103203	0.80110074E-04
9.7386063	0.11040133E-04	12.146873	0.77850236E-04
9.7595319	0.15075166E-04	12.209650	0.83751799E-04
9.7477044	0.37350712E-05	12.254231	0.70212456E-04
9.7504338	0.87334469E-05	12.296082	0.64133728E-04
9.7568025	0.95180909E-05	12.325196	0.61417198E-04
9.7622614	0.19933818E-04	12.342483	0.57574686E-04
9.7777281	0.93503747E-05	9.5757503	0.77125828E-04
9.7731791	0.17951145E-05	12.704587	0.84940773E-04
9.7786380	0.84440774E-05	12.752807	0.77669134E-04
9.7868262	0.14115719E-04	12.797388	0.85090379E-04
9.7813674	0.19131457E-05	12.842878	0.91799027E-04
9.7850066	0.24303100E-05	12.909294	0.91113989E-04
9.7950145	0.12645250E-04	12.958424	0.87724232E-04
9.7968342	0.43988100E-05	13.015742	0.91657295E-04
9.7950145	0.61940819E-05	13.075789	0.86554943E-04
9.7977440	0.60645546E-05	13.114911	0.79763618E-04
9.8050224	0.71054974E-05	13.156763	0.86110062E-04
9.8095715	0.52429028E-05	13.217720	0.97936809E-04
9.7804576	0.61763654E-05	13.276857	0.96413190E-04
9.7813674	0.14226349E-04	13.342364	0.95125791E-04
9.7804576	0.11822023E-04	13.406050	0.97696652E-04
9.7968342	0.15748787E-04	13.459729	0.91995877E-04
9.8050224	0.24609793E-04	13.513408	0.82110070E-04
9.8195794	0.17135005E-04	13.560718	0.83984082E-04
9.8032028	0.77669134E-05	13.613487	0.87476201E-04
9.8032028	0.98507674E-05	13.667166	0.94062801E-04
9.8268579	0.20279486E-04	13.722664	0.98456493E-04
9.8496031	0.20324368E-04	14.012894	0.81507709E-04
9.8514228	0.50755803E-05	14.069302	0.39936927E-04
11.060560	0.21803105E-04	13.725394	0.55417210E-03
11.062380	0.80696687E-04	13.774524	0.28384588E-03
11.096953	0.88901395E-04	13.931011	0.25520814E-03
11.140624	0.68696711E-04	14.081129	0.22632631E-03

Specimen 83289 (Second Proof Test, R=.25, ν=1 Hz, t_H=10 sec)

ΔK	da/dN	ΔK	da/dN
14.359531	0.16236975E-03	17.503835	0.16216896E-03
14.449603	0.13773988E-03	17.564792	0.16439730E-03
14.510560	0.11799976E-03	17.627569	0.19224764E-03
14.570607	0.11170450E-03	17.703083	0.20194447E-03
14.647031	0.12144464E-03	17.783146	0.20551927E-03
14.742561	0.13218871E-03	17.877767	0.20424368E-03
14.842640	0.13134225E-03	17.962379	0.20477518E-03
14.925433	0.12788950E-03	18.033344	0.20538147E-03
15.012775	0.12346432E-03	18.105219	0.19379095E-03
15.092838	0.12529108E-03	18.186192	0.20825548E-03
15.184729	0.12902336E-03	18.278993	0.21360587E-03
15.286628	0.13247611E-03	18.371793	0.22461372E-03
15.382158	0.13970050E-03	18.460045	0.22006255E-03
15.484966	0.14270444E-03	18.549206	0.21486571E-03
14.448693	0.22709403E-04	18.646556	0.21633814E-03
14.414120	0.26082231E-04	18.731168	0.21813342E-03
14.463250	0.86078566E-04	18.825789	0.22385781E-03
14.556960	0.11127930E-03	18.914040	0.23236173E-03
14.637023	0.12012574E-03	19.022308	0.23813731E-03
14.723455	0.12584620E-03	19.137853	0.23318850E-03
14.821715	0.12479502E-03	19.237933	0.23875541E-03
14.901778	0.11966511E-03	19.328922	0.22896410E-03
14.978202	0.11915330E-03	19.439001	0.23054284E-03
15.071913	0.12270841E-03	19.536350	0.23260189E-03
15.148337	0.12481864E-03	19.653716	0.24056250E-03
15.240227	0.13082257E-03	19.771081	0.24128298E-03
15.344856	0.13948791E-03	19.872070	0.23469244E-03
15.448574	0.13904303E-03	19.986706	0.24292864E-03
15.556841	0.13973200E-03	20.096793	0.24705462E-03
15.666019	0.14017294E-03	20.216888	0.24826721E-03
15.764278	0.13651941E-03	20.345171	0.25256642E-03
15.867087	0.13977924E-03	20.468906	0.25299555E-03
15.973534	0.14208239E-03	20.587181	0.25893648E-03
16.088170	0.14489341E-03	20.717284	0.26015695E-03
16.200077	0.15164930E-03	20.841928	0.27507425E-03
16.322901	0.16039338E-03	20.990227	0.29486948E-03
16.452094	0.16968863E-03	21.150353	0.30531040E-03
16.534887	0.17641697E-03	21.317758	0.30379860E-03
16.624048	0.19575945E-03	21.477885	0.30285765E-03
16.729586	0.18638151E-03	21.643470	0.30936551E-03
16.796003	0.17344453E-03	21.800867	0.29999152E-03
16.858779	0.17692090E-03	21.961904	0.31017260E-03
16.919737	0.17616893E-03	22.141136	0.31699148E-03
16.978874	0.17162170E-03	22.325828	0.32900327E-03
17.034373	0.17344059E-03	22.511429	0.33371586E-03
17.111707	0.19096418E-03	22.710677	0.33447176E-03
17.182672	0.19263740E-03	22.917204	0.33157019E-03
17.253637	0.17751145E-03	23.112813	0.31678676E-03
17.321873	0.17065320E-03	23.302964	0.31501511E-03
17.381010	0.17100359E-03	23.481286	0.31123559E-03

Specimen 83289 (Second Proof Test, R=.25, ν=1 Hz, t_H=10 sec)

ΔK	da/dN
23.876144	0.33266468E-03
24.095408	0.35427881E-03
24.334688	0.37565672E-03
24.585796	0.39255432E-03
24.862378	0.40555036E-03
25.152607	0.41334562E-03
25.457394	0.41677081E-03
25.743074	0.42094403E-03
26.048770	0.42637709E-03
26.370843	0.42716449E-03
26.702924	0.43712510E-03
27.052291	0.43921171E-03
27.405297	0.43925108E-03
27.748295	0.43736132E-03
28.108580	0.45495971E-03
28.501618	0.47499904E-03
28.916491	0.49358168E-03
29.377765	0.51964462E-03
29.881800	0.52881783E-03
30.391293	0.53618002E-03
30.908975	0.53964458E-03
31.433936	0.56436893E-03
32.015304	0.58826652E-03
32.670368	0.60369956E-03
33.386388	0.61684914E-03
34.120605	0.60216413E-03
34.822978	0.59188856E-03
35.481680	0.58995943E-03
36.189513	0.62716408E-03
37.021079	0.68621908E-03
38.016411	0.74106149E-03
39.176419	0.79708500E-03
40.430137	0.83464398E-03
41.779385	0.86613998E-03
43.244179	0.88704545E-03
44.847265	0.91527374E-03
46.812454	0.84704553E-03

NOTE: All of above data (83264D, 83266G, 83270B, 83270, 83288, and 83289) is in English Units. ΔK = Ksi $\sqrt{\text{inches}}$, da/dN = inches/cycle.

Constant ΔK
IN 718 da/dN Data, Variable Frequency

(T=1200F, R=0.1, No Hold Time)

ΔK=22.745 Ksi $\sqrt{in}$ K_{max}=25.3 Ksi $\sqrt{in}$

(Hz)	da/dN (in/cycle)
0.001	6.69 E-4
0.005	1.50 E-4
0.01	9.45 E-5
0.025	7.09 E-5
0.05	4.72 E-5
0.1	2.91 E-5
0.25	2.49 E-5
0.5	2.15 E-5
0.75	1.38 E-5
1.0	1.50 E-5
2.5	9.84 E-6
5.0	9.06 E-6
10.0	5.98 E-6

ΔK=32.75 Ksi $\sqrt{in}$ K_{max}=36.4 Ksi $\sqrt{in}$

(Hz)	da/dN (in/cycle)
0.001	2.05 E-3
0.005	4.72 E-4
0.01	2.17 E-4
0.025	1.34 E-4
0.05	9.06 E-5
0.1	7.09 E-5
0.25	5.51 E-5
0.5	4.33 E-5
0.75	3.35 E-5
1.0	3.39 E-5
2.5	2.52 E-5
5.0	2.09 E-5
10.0	1.61 E-5

Constant ΔK
IN 718 da/dN Data, Variable Hold Time

(T=1200F, R=0.1, ν =1Hz)

ΔK=22.745 Ksi $\sqrt{in}$ K_{max}=25.3 Ksi $\sqrt{in}$

Hold Time (s)	da/dN (in/cycle)
0.0	1.65 E-5
10.0	7.48 E-5
25.0	1.61 E-4
50.0	2.80 E-4
200.0	1.02 E-3
500.0	2.80 E-3

ΔK=32.75 Ksi $\sqrt{in}$ K_{max}=36.4 Ksi $\sqrt{in}$

Hold Time (s)	da/dN (in/cycle)
0.0	3.78 E-5
1.0	5.08 E-5
4.0	8.86 E-5
10.0	1.93 E-4
30.0	4.76 E-4
50.0	7.18 E-4
100.0	1.10 E-3
200.0	2.14 E-3
300.0	3.94 E-3
500.0	6.65 E-3

Appendix B: FORTRAN Code For SINH Interpolative Model

```
      PROGRAM SINH718
C
C     THIS PROGRAM GENERATES THE CONSTANTS FOR THE HYPERBOLIC
C     SINE EQUATION AND COMPUTES CRACK GROWTH RATES FOR
C     DESIRED STRESS INTENSITY RANGES.  THE MODEL IS ISOTHERMAL
C     (1200F), AND IS SPECIFIC TO INCONEL 718.  REQUIRED INPUTS
C     ARE STRESS RATIO, FREQUENCY (HZ), AND HOLD TIME (SEC).
C
C     READ INPUT
C
 10   PRINT *,'INPUT STRESS RATIO:'
      READ *,R
      PRINT *,'INPUT FREQUENCY (HZ):'
      READ *,FREQ
      PRINT *,'INPUT HOLD TIME (SEC):'
      READ *,THOLD
C
C     SINH CONSTANT C1
C
      C1=.5
C
C     SINH CONSTANT C2
C
      C2=3.197-1.1675*ALOG10((1.-R)/.9)-.1505*ALOG10(FREQ)
     *+.2053*ALOG10(THOLD+1.)
C
C     SINH CONSTANT C3
C
      C3=-1.721-.6243*ALOG10((1.-R)/.9)+.00717*ALOG10(FREQ)
     *+.0677*ALOG10(THOLD+1.))
C
C     SINH CONSTANT C4
C
      C4=-3.935+1.0131*ALOG10((1.-R)/.9)-.523*ALOG10(FREQ)
     *+.8127*ALOG10(THOLD+1.))
C
C     OUTPUT
C
      PRINT 20,C1,C2,C3,C4
 20   FORMAT(//2X,'C1=',F10.4,/2X,'C2=',F10.4,/2X,'C3=',F10.4,
     */2X,'C4=',F10.4)
      PRINT *,'      R         FREQ      THOLD'
      PRINT 30,R,FREQ,THOLD
 30   FORMAT(2X,3F10.4,//)
      PRINT *,'DESIRE DA/DN VALUES? 1 FOR YES, 0 FOR NO'
      READ *,IFLAG
      IF(IFLAG.EQ.0) GOTO 50
 40   PRINT *,'INPUT DESIRED DELTA K (KSI ROOT IN)'
      READ *,DK
```

```
      DADN=10**(C1*SINH(C2*(ALOG10(DK)+C3))+C4)
      PRINT 42,DADN,DK
42    FORMAT(2X,'CRACK GROWTH RATE IN IN/CYCLE IS:',
     *   E12.5,3X,'FOR DK=',F6.2,/)
      PRINT *,'ANOTHER DA/DN VALUE? 1 FOR YES, 0 FOR NO'
      READ *,JFLAG
      IF(JFLAG.EQ.1) GOTO 40
50    PRINT *,'CHANGE TEST PARAMETERS? 1 FOR YES, 0 FOR NO'
      READ *,KFLAG
      IF(KFLAG.EQ.1) GOTO 10
      STOP
      END
```

Appendix C: FORTRAN Code For MSE Interpolative Model

```
      PROGRAM MSE718
C
C     THIS PROGRAM GENERATES THE CONSTANTS FOR THE MODIFIED
C     SIGMOIDAL EQUATION, AND COMPUTES CRACK GROWTH RATES
C     FOR DESIRED STRESS INTENSITY RANGES.  THE MODEL IS ISOTHERMAL
C     (1200F), AND IS SPECIFIC TO INCONEL 718.  REQUIRED INPUTS ARE
C     STRESS RATIO, FREQUENCY (HZ), AND HOLD TIME (SEC).
C
C     READ INPUT
C
 10   PRINT *,'INPUT STRESS RATIO:'
      READ *,R
      PRINT *,'INPUT FREQUENCY (HZ):'
      READ *,FREQ
      PRINT *,'INPUT HOLD TIME (SEC):'
      READ *,THOLD
C
C     UPPER ASYMTOTE (ASSUMED CONSTANT)
C
      DKC=109.9
C
C     LOWER ASYMTOTE
C
      DKSTAR=10**(1.07918-.048646*ALOG10(FREQ)
     *+.05675*ALOG10(THOLD+1.))
C
C     VERTICAL LOCATION OF INFLECTION POINT
C
      DADNI=10.0**(-3.935+1.0131*ALOG10((1.-R)/.9)-.523*ALOG10(FREQ)
     *+.8127*ALOG10(THOLD+1.))
C
C     HORIZONTAL LOCATION OF INFLECTION POINT
C
      DKI=10.0**(1.721+.6243*ALOG10((1.-R)/.9)-.00717*ALOG10(FREQ)
     *-.0677*ALOG10(THOLD+1.))
C
C     SLOPE OF INFLECTION POINT
C
      DADNIP=1.7-1.8451*ALOG10((1.-R)/.9)-.2185*ALOG10(FREQ)
     *+.1956*ALOG10(THOLD+1.)
C
C     LOWER SHAPING COEFFICIENT (ASSUMED CONSTANT)
C
      Q=1.0
C
C     UPPER SHAPING COEFFICIENT
C
      D=-(SQRT(Q)*ALOG(DKI/DKC)/ALOG(DKI/DKSTAR))**2
C
```

```
C         OTHER COEFFICIENTS B' AND P
C
          CONST=ALOG(DKI/DKSTAR)
          CONST1=ALOG(DKC/DKI)
          BPRIME=ALOG(DADNI)-Q*ALOG(CONST)-D*ALOG(CONST1)
          P=DADNIP-Q/CONST+D/CONST1
C
C         OUTPUT
C
          PRINT 20,BPRIME,P,Q,D,DKSTAR,DKC,DADNI,DADNIP
 20       FORMAT(//2X,'B''=',F10.4,/2X,'P=',F10.4,/2X,'Q=',F10.4,
     *    /2X,'D=',F10.4,/2X,'DELTA K*=',F10.4,/2X,'DELTA KC=',
     *    F10.4,/2X,'DA/DNI=',E15.5,/2X,'DA/DNI''=',F10.4,//)
          PRINT *,'      R          FREQ      THOLD'
          PRINT 30,R,FREQ,THOLD
 30       FORMAT(2X,3F10.4,//)
          PRINT *,'DESIRE DA/DN VALUES? 1 FOR YES, 0 FOR NO'
          READ *,IFLAG
          IF(IFLAG.EQ.0) GOTO 50
 40       PRINT *,'INPUT DESIRED DELTA K (KSI ROOT IN)'
          READ *,DK
          DADN=EXP(BPRIME)*((DK/DKI)**P)*(ALOG(DK/DKSTAR)**Q)
     *    *(ALOG(DKC/DK)**D)
          PRINT 42,DADN,DK
 42       FORMAT(2X,'CRACK GROWTH RATE IN IN/CYCLE IS:',
     *    E12.5,3X,'FOR DK=',F6.2,/)
          PRINT *,'ANOTHER DA/DN VALUE? 1 FOR YES, 0 FOR NO'
          READ *,JFLAG
          IF(JFLAG.EQ.1) GOTO 40
 50       PRINT *,'CHANGE TEST PARAMETERS? 1 FOR YES, 0 FOR NO'
          READ *,KFLAG
          IF(KFLAG.EQ.1) GOTO 10
          STOP
          END
```

Bibliography

1. Larsen, J. M. and T. Nicholas. "Cumulative Damage Modeling of Fatigue Crack Growth," Proceedings of the AGARD Specialists Meeting of the Propulsion and Energetics Panel on Engine Cyclic Durability by Analysis and Testing, Lisse, Netherlands, 1984.

2. Broek, D. Elementary Engineering Fracture Mechanics. Third Edition, London, Martinue Nijhoff Publishers, 1982.

3. Larsen J. M., B. J. Schwartz, and C. G. Annis, Jr.. Pratt and Whitney Aircraft, Cumulative Damage Fracture Mechanics Under Engine Spectra, Air Force Materials Laboratory Report AFML-TR-79-4159, Wright-Patterson Air Force Base, Ohio, Jan 1980.

4. Thesis
Christoff, 2Lt Jeffery R. Evaluation of Fatigue-Creep Crack Growth in an Engine Alloy. MS thesis, AFIT/GA/AA/83D-2. School of Engineering, Air Force Institute of Technology (AU), Wright-Patterson AFB, OH, December 1983 (AD A136956).

5. Schwartz B. J., J. M. Larsen, and C. G. Annis. Pratt and Whitney Aircraft Co. "Cumulative Damage Fracture Mechanics Under Engine Spectra: FORTRAN User's Manual for Super SINH," Prepared for Air Force Materials Laboratory Contract F33615-77-C-5153, Pratt and Whitney Aircraft/Government Products Division, Jaurnary 1980.

6. Utah, David A. General Electric Co., "Crack Growth Modeling in an Advanced Powder Metallurgy Alloy," Air Force Wright Aeronautical Laboratories Report AFWL-TR-80-4098, Wright-Patterson Air Force Base, Ohio, Feb 1980.

7. Annual Book of ASTM Standards, Part 10 E647-81. "Standard Test Method for Constant-Load-Amplitude Fatigue Crack Growth Rates Above 10^{-8} m/Cycle," American Society for Testing of Materials, Philadelphia, Pennsylvania, July 1981.

8. Annual Book of ASTM Standards, Part 10 E399-81. "Standard Test Method for Plane-Strain Fracture Toughness of Metallic Materials," American Society for Testing and Materials, Philadelphia, Pennsylvania, July 1981.

9. Maxwell, D. C., J. P. Gallagher, and N. E. Ashbaugh. "Evaluation of COD Compliance Determined Crack Growth Rates," Air Force Wright Aeronautics Laboratory Report AFWAL-TR-84-4062, Wright-Patterson Air Force Base, Ohio, Jun 1984.

10. Shahinian P. and K. Sadananda. "Effects of Stress Ratio and Hold-Time on Fatigue Crack Growth in Alloy 718," Journal of Engineering Materials and Technology, Vol. 101: 224-230 (July 1979).

Vita

Gerald O'Neal Painter was born on 15 July 1954 in Jasper, Alabama. He graduated from Theodore High School in Mobile, Alabama in 1972. He attended Mobile College and The University of South Alabama, both in Mobile, in 1972 and 1973. He put education aside for a while, and was married later in 1973. In 1975, he enlisted in the United States Air Force, with his first child, a girl, born soon thereafter. His first assignment was at Keesler AFB, Mississippi, where he served as a radar repairman. In 1978, he entered the Airmens Education and Commissioning Program at Auburn University, Auburn, Alabama, where he received a Bachelor's Degree in Mechanical Engineering in 1980. His second child, a boy, came in 1978, while at Auburn. He was commissioned a Second Lieutenant through Officer's Training School at Lackland AFB, Texas on 11 December 1980. He served at the Air Force Armament Laboratory, Eglin AFB, Florida, in the Bombs and Warheads Branch, until he entered the School of Engineering, Air Force Institute of Technology, in June 1983.

Permanent Address: 8002 Quimby Drive
Mobile, Al 36619

UNCLASSIFIED

SECURITY CLASSIFICATION OF THIS PAGE

REPORT DOCUMENTATION PAGE

1a. REPORT SECURITY CLASSIFICATION UNCLASSIFIED	1b. RESTRICTIVE MARKINGS
2a. SECURITY CLASSIFICATION AUTHORITY 2b. DECLASSIFICATION/DOWNGRADING SCHEDULE	3. DISTRIBUTION/AVAILABILITY OF REPORT Approved for public release, distribution unlimited.
4. PERFORMING ORGANIZATION REPORT NUMBER(S) AFIT/GAE/AA/84D-20	5. MONITORING ORGANIZATION REPORT NUMBER(S)
6a. NAME OF PERFORMING ORGANIZATION School of Engineering Air Force Inst. of Technology 6b. OFFICE SYMBOL (If applicable) AFIT/EN	7a. NAME OF MONITORING ORGANIZATION
6c. ADDRESS (City, State and ZIP Code) Air Force Institute of Technology Wright-Patterson AFB, OH 45433	7b. ADDRESS (City, State and ZIP Code)
8a. NAME OF FUNDING/SPONSORING ORGANIZATION 8b. OFFICE SYMBOL (If applicable)	9. PROCUREMENT INSTRUMENT IDENTIFICATION NUMBER
8c. ADDRESS (City, State and ZIP Code)	10. SOURCE OF FUNDING NOS. PROGRAM ELEMENT NO. | PROJECT NO. | TASK NO. | WORK UNIT NO.
11. TITLE (Include Security Classification) See Box 19	
12. PERSONAL AUTHOR(S) Gerald O. Painter, B.M.E, 1Lt, USAF	
13a. TYPE OF REPORT MS Thesis 13b. TIME COVERED FROM ____ TO ____	14. DATE OF REPORT (Yr., Mo., Day) 84 December 15. PAGE COUNT 71
16. SUPPLEMENTARY NOTATION	

17. COSATI CODES

FIELD	GROUP	SUB. GR.
20	11	

18. SUBJECT TERMS (Continue on reverse if necessary and identify by block number)

Fatigue, crack growth, high temperature fracture, Charts, Table (Data), Computer Programs.

19. ABSTRACT (Continue on reverse if necessary and identify by block number)

Title: EVALUATION OF INTERPOLATIVE MODELING CONCEPTS FOR FATIGUE CRACK GROWTH AT ELEVATED TEMPERATURE

Thesis Chairman: George Haritos, Major, USAF

Approved for public release: IAW AFR 190-17.
LYNN E. WOLAVER 21 Feb 85
Dean for Research and Professional Development
Air Force Institute of Technology (ATC)
Wright-Patterson AFB OH 45433

20. DISTRIBUTION/AVAILABILITY OF ABSTRACT UNCLASSIFIED/UNLIMITED ☒ SAME AS RPT. ☐ DTIC USERS ☐	21. ABSTRACT SECURITY CLASSIFICATION UNCLASSIFIED
22a. NAME OF RESPONSIBLE INDIVIDUAL George K. Haritos, Major, USAF	22b. TELEPHONE NUMBER (Include Area Code) 513-255-2998 22c. OFFICE SYMBOL AFIT/ENY

DD FORM 1473, 83 APR EDITION OF 1 JAN 73 IS OBSOLETE.

UNCLASSIFIED

SECURITY CLASSIFICATION OF THIS PAGE

This thesis ~~work~~ presents an examination of interpolative schemes for fatigue crack growth at elevated temperature (1200°F). An interpolative scheme involving the linear superposition of effects due to stress ratio, loading frequency, and peak load dwell or hold time, is applied to two state-of-the-art crack growth rate prediction models. These models are the SINH model, developed by Pratt and Whitney Aircraft, and the MSE model, developed by General Electric. SINH model is based on the hyperbolic sine function, and MSE model is based on a sigmoidal equation.

The results of an experimental program are presented. Fatigue crack growth rate tests are performed on compact tension specimens according to ASTM standards. Two interpolative models are developed from the resulting data base. Additional tests are performed and the model predictions are compared to these additional tests.

It is found that linear (on log-log scale) functional forms can be assumed to relate model constants to the test parameters (load ratio, frequency, and hold time). Also, it is found that these functional forms can be applied to both models. More work is needed to determine whether the effects of variations in each of the test parameters on crack growth rate are independent of each other and can be linearly superimposed.

When the same functional forms are applied to the SINH and the MSE models, they behave much alike. Originator-supplied key words included.